ifo WORKING PAPERS

307
2019

July 2019

A Framework for Modeling the Dynamics of Power Markets – The EU-REGEN Model

Christoph Weissbart, Geoffrey J. Blanford

ifo INSTITUTE

Leibniz Institute for Economic Research
at the University of Munich

Imprint:

ifo Working Papers
Publisher and distributor: ifo Institute – Leibniz Institute for Economic Research at the University of Munich
Poschingerstr. 5, 81679 Munich, Germany
Telephone +49(0)89 9224 0, Telefax +49(0)89 985369, email ifo@ifo.de
www.ifo.de

An electronic version of the paper may be downloaded from the ifo website:
www.ifo.de

ifo Working Paper No. 307

A Framework for Modeling the Dynamics of Power Markets – The EU-REGEN Model

Abstract

The long-run development of power markets will be deeply affected by the gradual substitution of fossil fuel-based generation technologies by renewable energy technologies (RES). However, the intermittent supply of RES, in combination with the temporal non-homogeneity of electricity demand, limits the competitiveness of renewable energies (Joskow, 2011). We develop a partial-equilibrium model of the European power market that contributes with a framework for capturing the temporal and spatial variability of RES. Furthermore, we differentiate wind and solar technologies by different quality classes and contribute with a routine for using meteorological data to approximate the temporal availability of renewable energy technologies. The composite of all these RES features allows then for a detailed representation of RES and their implicit substitution elasticity with fossil fuel-based technologies. Our results for the long-run electricity generation path of the European power market show that, under an 80% CO_2 emissions reduction scenario until 2050, renewable energy technologies become the main technologies that will meet the demand. The 2050 generation share of wind and solar power combined is around 40%. However, with the detailed depiction of their temporal and spatial characteristics, we identify that gas power is necessary as a complement to compensate for their intermittent supply, which requires in turn the utilization of carbon capture and storage to adhere to the climate target.

JEL code: C61, L94, Q41, Q42

Keywords: European power market, renewable energies, energy modeling, investment planning

Christoph Weissbart*
ifo Institute – Leibniz Institute for Economic Research
at the University of Munich
Poschingerstr. 5
81679 Munich, Germany
Phone: + 49 89 9224 1256
weissbart@ifo.de

Geoffrey J. Blanford
Electric Power Research Institute
3420 Hillview Avenue
Palo Alto, California 94304, USA
igblanford@epri.com

* Corresponding author.

1. Introduction

Since the beginning of the century, the energy policy of the European Union (EU) was mainly driven by the decarbonization of the supply side. The *power market* will be one of the main leverages to reach the ambitious decarbonization targets. On the one hand, electrification of other energy sectors and the conversion of power to other energy commodities (e.g., power-to-gas) will result in increasing demand (EC, 2011a, 2014). On the other hand, the electricity generation mix has to reduce its CO_2 intensity. Therefore, renewable energy sources (RES) have to become the major source to meet this load. Their potential, especially for variable RES, is vast, and future cost estimates suggest economic viability (e.g., Coppens et al., 2009; Marcel Šúri et al., 2007; IRENA, 2016).[1] Yet, variable RES are spatially dispersed and their quality varies temporally. This means that a cost-efficient realization of EU decarbonization will require the integration of national power markets and EU-wide cooperation on climate and energy policy.

In 2008, the European Commission (EC) introduced the "Energy & Climate Package" with its "20-20-20" targets (EC, 2007). Comprising a 20% share of RES in energy consumption, a 20% reduction of greenhouse gas (GHG) emissions compared to 1990 levels, and a 20% reduction of final energy consumption compared to a business-as-usual scenario. Furthermore, each member state had to translate those EU-wide targets into national targets. To address the mid-term and long-term perspective, the European Commission released "A roadmap for Moving to a Competitive Low Carbon Economy in 2050" (EC, 2011a,b), emphasizing a GHG emission reduction target of at least 80% compared to 1990 levels. In 2014, this decarbonization path was further specified by targets for 2030: a 27% share of RES in energy consumption, a 40% reduction of GHG emissions compared to 1990 levels, and a 27% decrease of final energy consumption. Currently, the EC updates its long-term target with now aiming for a carbon-free economy by 2050 (EC, 2018).

Existing models for the European power market already provide insight into the sector's future development under current RES and CO_2 emission targets. The LIMES-EU_+ model is used in Knopf et al. (2015) and Schmid and Knopf (2015) to look into the impact of the EC's RES generation targets for 2030 and the relationship between transmission capacity and RES capacity additions. Similarly, Schaber et al. (2012) analyze the impact of transmission capacity expansion for variable RES integration and quantify advantages and costs by means of the URBS-EU model. Kunz and Zerrahn (2016) apply the stochastic version of the ELMOD model to address the topic of congestion management between neighboring countries. Also the EMPIRE model considers

[1] See, e.g., Huber and Weissbart (2015) for estimates on the variable RES potential in other regions of the world.

uncertainty by stochastic optimization. In Brovold et al. (2014), the dispatch of hydro power is optimized under uncertainty with respect to meteorological circumstances. Moreover, the future role of nuclear power is examined in Aune et al. (2015). They use the LIBEMOD model to calculate the eoconomic costs of a phase-out of nuclear power by 2030. The economics of variable RES are further analyzed with the EMMA model in Hirth (2013) by emphasizing their market value. With a different focus, Deane et al. (2012) link results from the PRIMES energy system model (Mantzos and Capros, 1998) to the PLEXOS power system modeling tool (Energy Exemplar, 2018) to conduct a detailed evaluation of different power system components. A broader perspective is taken by Richter (2011) and Henning and Palzer (2014). The DIMENSION model focuses on the European power markets' interaction with the heat and transportation sector (Richter, 2011). A pure German perspective is taken in the REMod model to, however, examine the impact of different climate targets on endogenous sector coupling (Henning and Palzer, 2014). The behavior of private investors is researched in Schröder et al. (2013). They use the EMELIE-ESY model to optimize a long-run generation capacity investment under the assumption of profit maximizing agents.[2]

Yet, we still see analysis on the role of RES along the targeted decarbonization path that allow room for improvements. To provide insights into the role of variable RES technologies over time, further developments of their depiction in numerical models is required to analyze the relative costs of different technologies that rely on the same resource. Furthermore, the trade-off between utilizing regional resource qualities versus system-wide averaging effects of variable RES needs to be analyzed in dynamic models. Concerning conventional generation technologies, to elaborate on the future role of existing and new capacities in the European power market remains of great importance, and understanding their contribution in the coming transition phase is crucial to design relevant policies.

For that purpose, we developed the framework of the *EU-REGEN model*. The model was built to generate quantitative scenarios that represent an optimal and consistent decarbonization path for the European power system towards 2050. EU-REGEN minimizes total system costs with respect to conventional and RES generation capacity investment, generation capacity conversion and retirement, generation dispatch and curtailment, transmission capacity investment, physical electricity exchange, storage capacity investment and operation, and carbon capture and storage (CCS) capacity investment and operation. The model is set up as a partial equilibrium model that

[2] See Savvidis et al. (2019) and Connolly et al. (2010); Bhattacharyya and Timilsina (2010); Foley et al. (2010); Teufel et al. (2013) for a more extensive overview of existing power market models and their applications.

assumes complete markets with perfect information and is subject to a wide range of constraints. Moreover, EU-REGEN is a deterministic and perfect foresight model. Meaning, there is no uncertainty about input parameters, for example, investment cost, fuel prices, and demand. The model is formulated as a linear optimization problem in GAMS (General Algebraic Modeling System) and solved with the CPLEX solver.

Among others, the optimization of investment into generation, storage, transmission, and CCS capacity is driven by costs for capacity additions and upper bounds on capacity additions and accumulation. Those bounds are derived from political and technical feasibility as well as geological and geographical potentials. Furthermore, electricity demand, which is determined exogenously in the model in this paper, has to be satisfied by the combination of generation, storage discharge, and electricity exchange at any time. Dispatch of generation capacity and system operation are driven by marginal costs, availability, and investment costs of capacities. In addition, EU-REGEN makes use of the duality theorem and derives electricity and CO_2 prices from the dual variables of the market-clearing constraint and the system-wide CO_2 market constraint, respectively.

One specific characteristic of the EU-REGEN model is the detailed representation of the variable RES wind and solar. We apply different resource-quality classes to both resources, which are reflected in separate temporal availability profiles and capacity potentials for each quality class. Moreover, certain technological progress is assumed by setting improved technical characteristics of wind and solar technologies in future time periods.

This paper provides an overview of the model set-up, the main assumptions, and a model application. We start with an introduction to the underlying economic rationale in Section 2. Then, Sections 3 and 4 present the model structure and resolution. This is followed by a detailed explanation of the methodology for modeling time profiles for variable RES, the aggregation of time segments, and showing the major parameter values in Sections 5, 6, and 7. Finally, the model application to two policy scenarios with respective results is introduced in Section 8. Section 9 concludes with a brief outlook.

2. Model structure

In this section, we present the basic structure of the model and relate this to the microeconomic concepts underlying power markets. EU-REGEN is a partial equilibrium model of an electricity system consisting of multiple regions connected via transmission lines. It comprises consumers, producing firms, and a central planner (or regulator). This results in a multi-period investment and dispatch model. The model's main output variables are electricity prices, carbon prices, investment and production quantities of generation technologies, and investment in transmission capacities.

2.1. Demand side

Consumers demand electricity and obtain utility from this. We assume that the respective demand function $d(p)$ is downward-sloped, that is, electricity is a normal good whose demand decreases in its market price p. Meaning, the lower the price for electricity, the higher is the market demand. The inverse of the demand function $p(q)$, which indicates the price, that is, the willingness to pay, as a function of the available quantity q. The change in demand as a reaction to a change in the price is determined by price elasticity ϵ.[3] The absolute value of ϵ indicates the degree of demand adjustment. However, for the remainder of this paper, we assume a price elasticity of $\epsilon \approx 0$ and thus demand is not reacting to price changes.[4]

2.2. Supply side

We assume a representative firm that invests in electricity generation capacity that is used to produce q quantities of electricity. Firms are assumed to be price takers and hence their objective is profit maximization. Furthermore, the production of electricity is subject to technical constraints, which limit the feasible production set. This results in the supply function $s(p)$, which equals the market supply when there is only one representative producer, as in the case of the EU-REGEN model. The supply function is then a mapping of quantity q to the minimal costs for the provision of this quantity. Taking again the inverse of this function $p(q) = s(p)^{-1}$ results in the relationship between quantities and prices.

2.3. Central planner and social welfare

The central planner invests in transmission infrastructure between regions and maximizes social welfare. Social welfare in a market is defined as the sum of consumers'

[3] The price elasticity is defined as the percentage change in quantity over the percentage change in price. This can be written as $\epsilon = \frac{\Delta q/q}{\Delta p/p}$.

[4] See Mier and Weissbart (2018) for a model set-up with responsive demand.

surplus CS and producers' surplus PS.[5] As shown in Figure 1a, the CS is characterized by the area between the demand curve and the horizontal line along the market clearing price and can be interpreted as the overall willingness to pay that is not appropriated by the producers. The graphical representation of the PS is the area between the horizontal line along the market clearing price and the supply curve. It can be interpreted as the overall revenue above the producers' costs or their profit. We assume that the assumptions of a competitive equilibrium hold and firms are price takers, have access to perfect information, are not subject to any uncertainty, and hence obtain zero profit. It has been shown that the social welfare is maximized under the conditions of a competitive market and thus the efficient market equilibrium is reached.

As introduced above, we assume that demand is perfectly inelastic, that is, it does not react to changes in the market price. This market equilibrium setting is depicted in Figure 1b. Under this assumption, the maximization of social welfare does not distort the consumption choice of consumers. Thus, the minimization of total costs yields the social welfare maximizing market equilibrium, which is the area below the supply curve in Figure 1b.

We assumed, in this section, for illustration purposes, that producers incur only marginal costs for producing electricity. In the following, we will point out the economic rationale of the underlying market equilibrium and the type of costs that are considered in the EU-REGEN model.

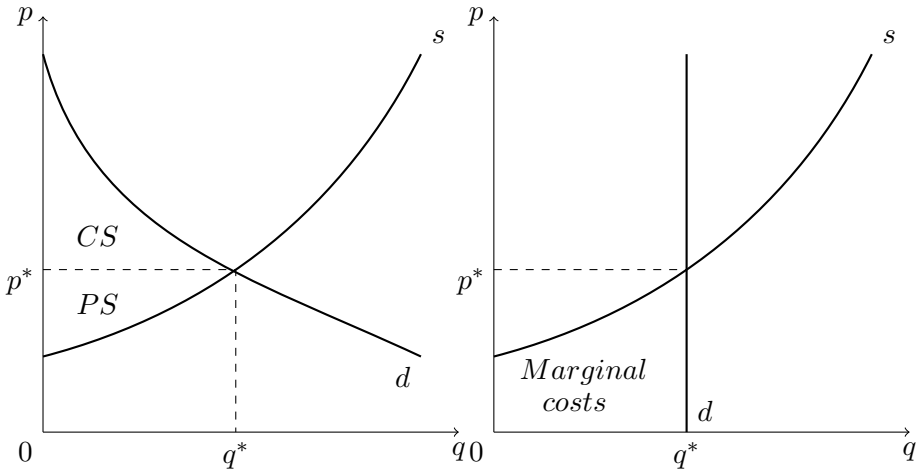

(a) Elastic demand (b) Perfectly inelastic demand

Figure 1: Market equilibrium under different demand elasticities

[5] Note that the social welfare is also known as the Marshallian aggregate surplus.

2.4. Market equilibrium

The long-run market equilibrium of the EU-REGEN model is based on the minimization of total system cost. The market value is the economic rationale underlying the solution to this problem (see Lamont, 2008; Borenstein, 2008; Hirth, 2013). This concept allows for a detailed depiction of RES, whose supply pattern is intermittent and exhibits a certain temporal correlation with demand.[6] This refers to the temporal non-homogeneity of electricity (Joskow, 2011).[7]

In brief, investment in capacity of a generation technology is cost-effective when its net market value is greater than the net market value of alternative generation technologies. The net market value is defined as the market value minus investment costs. Economic theory generally defines the market value mv, or marginal value, of a technology as the difference between the actual market price p^t and the variable costs of the technology VC. In the case of variable RES, the variable costs are close to zero. Hence, the annual market value of a generation technology is characterized by the sum over the differences between the market price and the variable costs multiplied by the hourly availability factor AV^t. For variable RES, the hourly availability factor AV^t represents the observed availability profile. In terms of generation technologies that are dispatchable,[8] this availability factor is assumed to be equal to 1 and can be dropped. Hence, the market value equals the weighted mean of the market price p^t that is corrected for the variable costs VC. This can be expressed with the time-weighted arithmetic mean of the marginal price:

$$mv = \sum_t ((price^t - VC) \cdot AV^t) = A((price^t - VC) \cdot AV^t) \cdot T. \tag{1}$$

Focusing on variable RES and thus neglecting the variable costs and keeping the availability factor, the capability to meet demand is another perspective on the market value. This means that a generation technology's long-term value is high when its availability profile allows for serving the market in times of high prices. In the analogy of Lamont (2008), the covariance can be used to divide the market value into two components. The covariance between the price and the hourly availability factor AF^t can be expressed as:

$$cov_{p,AV} = A(p^t \cdot AF^t) - A(p^t) \cdot A(AF^t). \tag{2}$$

[6] A technology is intermittent when the temporal output variation is driven by exogenous factors.

[7] Note that the economic viability of different generation technologies can also be evaluated with a lower degree of detail, e.g., levelized costs of electricity generation (LCOE) (Kost et al., 2013) or average cost functions (Stoft, 2002).

[8] A technology is dispatchable when there is temporal control over it.

Rearranging Equation (2) and substituting $cov_{p,AF} + A(p) \cdot A(AF^t)$ into (1) brings us to the following definition of the market value:

$$mv = A(p^t) \cdot A(AF^t) \cdot T + cov_{p,AV} \cdot T. \tag{3}$$

Equation (3) contains both components of the market value. The first term is the energy value and the second part is the demand matching capability. The energy value indicates that, in this case, the market value of an intermittent generation technology depends, on the one hand, on the amount of energy that can be provided by adding one unit of capacity. On the other hand, the demand-matching capability comprises the value of serving the market in times of high prices and hence contributes to a reduction in this price with the low marginal costs of variable RES.

Correcting the market value for the fixed costs FC and investment costs IC yields the net market value nmv by:

$$nmv = mv - IC - FC = A(p^t) \cdot A(AF^t) \cdot T + cov_{p,AF} \cdot T - IC - FC. \tag{4}$$

With respect to the market equilibrium of the EU-REGEN model, this means that the optimal investment decision in each time period is determined in the order of the net market value of technologies and by the set of constraints that defines the feasible production set. Moreover, it is important to emphasize that market value is a dynamic concept. The investment decision of previous periods impacts market prices in a period and hence the market value of technologies.

2.5. Elements of system costs

As mentioned above, total costs in a market serve as a measure for global welfare under the assumption of perfectly inelastic demand. With respect to power markets, these costs are referred to as total system costs. They comprise the costs for providing electricity to the market as well as the investment costs for the underlying generation and transmission infrastructure. Moreover, costs can be differentiated between private and social costs.

Private costs

The EU-REGEN model covers all costs that a representative firm incurs for generating electricity. However, the composition of private costs for producing electricity varies with the type of generation technology.[9] In general, we can differentiate technologies along two dimensions: RES-based/fossil fuel-based technologies and intermit-

[9] Private costs are understood as all costs that firms take into account when maximizing their profits.

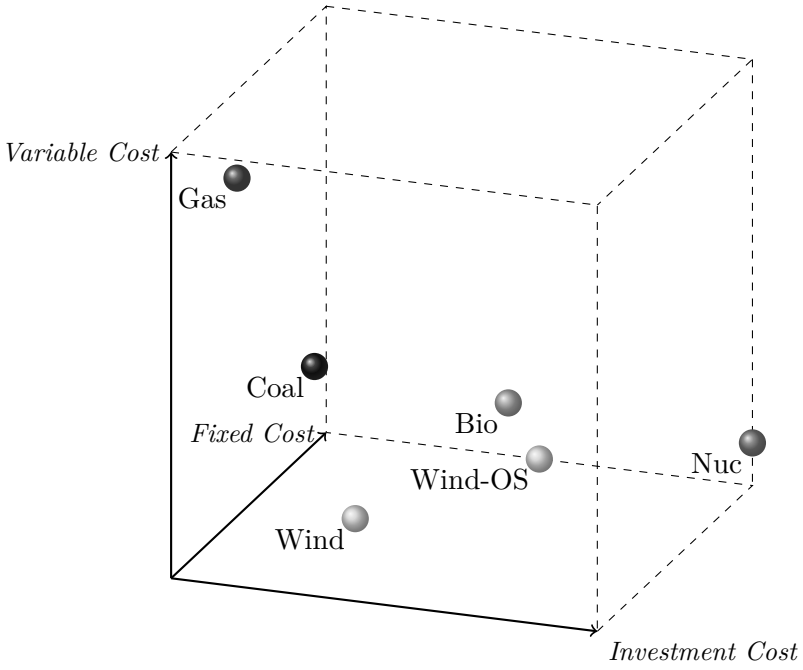

Figure 2: Magnitude of cost types by generation technology

tent/dispatchable technologies. Costs occurring with the production of electricity can be differentiated into investment cost, variable cost, and fixed cost.[10]

Yet, different generation technologies cause each of these costs to a varying extent. Whereas dispatchable technologies are subject to all three kinds of costs, intermittent generation technologies induce negligible variable cost. Figure 2 indicates the relevance of investment, variable, and fixed costs for major generation technologies. This is done by locating each technology in the space of investment costs, variable costs, and fixed costs. We look at the standard generation technologies: biomass, coal, gas, nuclear, and wind. The magnitude of each cost component is based on Schröder et al. (2013).

Electricity generation from biomass is subject to relatively high investment cost and moderate variable and fixed cost. The latter is comparably high for nuclear power, which also triggers very high investment cost and moderate variable cost. In contrast, gas power induces low investment cost, yet, causes high variable cost from fuel sourcing. These costs are comparably lower for coal power, which is subject to low investment and fixed cost as well. The former type of costs is higher for wind power, which, however, hardly causes variable and fixed costs. Concerning wind power, its cost is furthermore

[10] Note that investment costs occur only once to create one additional unit of electricity generation capacity, whereas fixed costs arise in each time period where a respective unit of capacity is active.

driven by geographic circumstances. For example, the composition of total costs for offshore wind power comprises higher investment and fixed costs.

Note that, as Figure 2 depicts, coal power has low costs with respect to all three cost components. Furthermore, this technology can be dispatched and is hence independent of meteorological and geographic circumstances. The high competitiveness of coal power, without considering its external costs and its high abundance, can be seen as the main driver for its dominating role across power markets all over the world (Steckel et al., 2015).

Social costs

With respect to social costs, the EU-REGEN framework includes policies that address the external effect from CO_2 emissions only. Yet, further environmental externalities, such as local air pollution from SO_2 as well as feedback effects on the power market are not considered. The same holds true for non-environmental externalities. Since the model setting does not represent the interaction between the power market and the rest of the economy, economic spillovers cannot be valued. Moreover, the EU-REGEN model yields the inter-temporal equilibrium by relying on perfect expectations. Consequently, the issue of technology lock-ins cannot be examined due to the perfect-foresight nature of the model. Similarly, the effects of market failure due to strategic investment and dispatch behavior cannot be evaluated in this model setting.

In general, externalities from electricity generation that cause social costs,[11] can be distinguished into environmental externalities and non-environmental externalities (Borenstein, 2012). Considering the social cost from environmental externalities that are not internalized by private firms can change a classification, as in Figure 2. There is scientific consensus that the emission of CO_2 into the atmosphere is one of the main drivers for the observed increase in global temperature (e.g., Cook et al., 2013, 2016). With power markets being one of the main emitters of CO_2, these emissions are one of the main environmental externalities from electricity generation.[12] If regulators introduce a policy instrument and hence producers internalize the social cost from CO_2 emissions, their variable cost for fossil fuel-based generation technologies will increase significantly. This mainly concerns coal power, which is highly competitive due to low private cost, but it suffers from high social cost due to its high carbon content.[13]

[11] Social costs are production-related costs that are not internalized by private firms per se.

[12] Note that electricity and heat production caused 42% of global CO_2 emissions from fuel combustion in 2016 (IEA, 2018).

[13] The carbon content is the amount of carbon embedded in the fuel itself. The contained carbon is released through the combustion of the fuel. Then, it reacts with oxygen, and results in CO_2.

Note that extant research shows that the impact of power markets on climate change (mainly from CO_2 emissions) yields a feedback effect as well. The impact of climate change on power markets itself can be distinguished into effects on demand and supply (Mideksa and Kallbekken, 2010). Power generation could be impacted by reduced water supply from heat waves and droughts, which would influence hydropower directly and thermal power plants indirectly through lack of cooling water and the reduced efficiencies resulting from that (Rübbelke and Vögele, 2011; Golombek et al., 2012).[14] Moreover, increasing mean temperatures from climate change could alter electricity demand through a stronger correlation with temperatures. An example would be the increased adoption of air conditioning and, thus, soaring electricity demand (Auffhammer and Mansur, 2014).

However, there are more sources of environmental damage from electricity generation. Local environmental damages can comprise, for example, environmental degradation through fossil fuel extraction, loss of biodiversity, and local air pollution from fossil fuel combustion (e.g., Edenhofer et al., 2013).[15] Concerning the latter, pollutants such as nitrogen oxide (NO_x) and sulfur dioxide (SO_2) can cause local air pollution and enhance acid rain and smog (Owen, 2004).

Non-environmental externalities from electricity generation can create negative as well as positive impacts. One of the most prominent (negative) non-environmental externalities are path dependencies. Path dependencies in the power market are understood as the costs of locking an energy system into a subset of technologies due to, for example, the underlying infrastructure (Fouquet, 2016). Since investment in production and transmission infrastructure are characterized by long amortization periods, they can lead to slow adoption in the market and thus create inefficiencies. Moreover, both conventional generation technologies and RES, exhibit a negative externality on landscape aesthetics and, hence, property values (Davis, 2011; Gibbons, 2015).[16] Especially wind power can entail an externality through having a negative impact on human well-being (e.g., Krekel and Zerrahn, 2017).

Though, it is important to emphasize that there exist positive externalities as well such as employment effects, knowledge spillovers, and learning effects, among others (Edenhofer et al., 2013; Fouquet, 2016). With respect to employment effects, the large-scale investment and deployment of a new generation technology, for example, solar

[14] Note that in terms of wind power, changing climatic conditions could alter the temporal and geographic structure of wind resources. Yet, it cannot be generalized whether this leads to an overall positive or negative impact (Pryor and Barthelmie, 2010).

[15] See Samadi (2017) for a general overview of externalities from electricity generation.

[16] See Mattmann et al. (2016a,b); Dröes and Koster (2016); Chiabrando et al. (2009); Gamble and Downing (1982) for estimates on the impact of single technologies.

power, can lead to additional jobs in the energy sector and, thus, have a positive impact on the overall economy.[17] Innovation market failures, for example, knowledge spillovers, and learning effects, occur when since single firms, in the private optimum, do not account for their impact on the knowledge stock of the economy and the development of future technology costs via their learning-by-doing (Fischer and Newell, 2008).

In this section, we described the general structure of the EU-REGEN model. Moreover, we outlined the type of costs that the framework considers for cost-minimization and, hence, a welfare-maximizing market outcome. In the following section, we will depict the numerical implementation of the cost-minimization problem with its set of constraints.

[17] Note that a higher number of workers in this sector is then mainly required due to the installation of capacities (Frondel et al., 2010). Thus, the nature of investments in RES, which are high up-front investment costs and low variable costs, questions to what extent this effect still holds in the long run (Borenstein, 2012).

3. Numerical implementation

The EU-REGEN model is a linear program based on the US-REGEN model (Blanford et al., 2014).[18] In the following, we present the algebra of the model and use subscripts to refer to region r, time period t, time segment s, vintage v, generation technology i, storage technology j, natural gas supply class n, and biomass supply class b. The nomenclature of the sets, variables, and parameters used in this section are described in Table A.7 in Appendix Appendix A.

System costs

The linear and deterministic optimization model minimizes the total discounted system cost c^{tot} (Equation (5)) that consists of investment costs for generation capacity $c^{\text{gc}}_{r,t}$, transmission capacity $c^{\text{tc}}_{r,t}$, storage capacity $c^{\text{sc}}_{r,t}$, costs from generation operation $c^{\text{vc}}_{r,t}$, maintenance costs for generation capacity $c^{\text{fom}}_{r,t}$, and operation and maintenance costs for transmission $c^{\text{tvo}}_{r,t}$ and $c^{\text{tfm}}_{r,t}$:

$$c^{tot} = \sum_{r,t}[(c^{\text{gc}}_{r,t} + c^{\text{tc}}_{r,t} + c^{\text{sc}}_{r,t}) \cdot tf_t + c^{\text{vc}}_{r,t} + c^{\text{fom}}_{r,t} + c^{\text{tvo}}_{r,t} + c^{\text{tfm}}_{r,t}] \cdot \text{DF}_t \tag{5}$$

This includes the investment tax factor tf_t, which is determined by the investment tax rate TK and the length of time step t in years YR_t as well as the discount factor DF_t (Equation (6)):

$$tf_t = \frac{(1 + \text{TK})}{\text{YR}_t} \qquad \forall t \in \mathcal{T} \tag{6}$$

In Equation (7), investment costs for generation capacity investments by firms $c^{\text{gc}}_{r,t}$ are defined as a function of the new generation capacity $gc^{\text{new}}_{i,r,t}$, its investment costs $\text{IC}^{\text{gc}}_{i,t}$, and the technology-specific lifetime factor $\text{LF}_{i,v,r,t}$. The latter one is applied to avoid end effects and adjusts investment costs for the share of the technology-specific lifetime that lies within the model horizon:

$$c^{\text{gc}}_{r,t} = \sum_{i \in \mathcal{I}_{\text{new}}} gc^{\text{new}}_{i,r,t} \cdot \sum_{v} \text{IC}^{\text{gc}}_{i,t} \cdot \text{LF}_{i,v,r,t} \qquad \forall r \in \mathcal{R}, t \in \mathcal{T} \tag{7}$$

Costs for new transmission capacity investment between regions undertaken by the central planner (Equation (8)) vary with the new transmission capacity $tc^{\text{new}}_{r,rr,t}$ and the region-specific investments costs $\text{IC}^{\text{tc}}_{r,rr}$ that are a function of the distance between the regions' load centers or other geographic considerations as, for example, overseas

[18] See Young et al. (2013) and Blanford et al. (2014) for detailed information on the U.S. Regional Economy, Greenhouse Gas, and Energy (US-REGEN) model and carried-out analyses. Furthermore, note that the US-REGEN framework also captures the interaction between the power sector and other sectors of the economy.

connections:

$$c^{\text{tc}}_{r,t} = \sum_{rr} tc^{\text{new}}_{r,rr,t} \cdot \text{IC}^{\text{tc}}_{r,rr} \qquad \forall r \in \mathcal{R}, t \in \mathcal{T} \tag{8}$$

The last component of investment costs, electricity storage charge and discharge capacity, is described in Equation (9) by the product of the added capacity $sc^{\text{new}}_{j,r,t}$ for storage technology j and the investment costs for storage charge capacity $\text{IC}^{\text{sc}}_{j}$:

$$c^{sc}_{r,t} = \sum_{j} sc^{\text{new}}_{j,r,t} \cdot \text{IC}^{\text{sc}}_{j} \qquad \forall r \in \mathcal{R}, t \in \mathcal{T} \tag{9}$$

Costs from electricity generation operation and maintenance (O&M) by firms are represented by $c^{\text{vc}}_{r,t}$ and $c^{\text{fom}}_{r,t}$, respectively. In Equation (10), the variable dispatch costs are the specific variable operation costs $mc_{i,v,r,t}$ times the actual generation $g_{s,i,v,r,t}$ and the number of hours in each load segment H_s (see Section 6). We include costs from biomass separately by accounting for the cost $\text{OC}^{\text{bio}}_{b,r}$ from biomass supply $bs_{b,r,t}$:

$$c^{\text{vc}}_{r,t} = \sum_{i,v}(mc_{i,v,r,t} \cdot \sum_{s}(g_{s,i,v,r,t} \cdot \text{H}_s)) + \sum_{b} bs_{b,r,t} \cdot \text{OC}^{\text{bio}}_{b,r} \qquad r \in \mathcal{R}, \forall t \in \mathcal{T} \tag{10}$$

A firm's marginal costs $mc_{i,v,r,t}$ comprise variable operation costs $\text{OC}^{\text{vom}}_{i,v,r}$, fuel costs, and costs from CO_2 permits (Equation (11)). Fuel costs vary with the fuel use coefficient $\text{FC}_{i,f}$ (a binary variable allocating fuel type to generation technology), the technology-specific heat rate $\text{HR}_{i,v,f,r}$ (with a lower heat rate indicating a more efficient combustion process), as well as time period and region-specific adjustment factors $\text{FT}_{f,t}$ and $\text{FR}_{f,r}$ (to account for, e.g., intra-regional fuel distribution costs). Costs from carbon permits are the product of emission intensity $\text{EM}_{i,v,r}$ and the permit price PC_t:

$$\begin{aligned} mc_{i,v,r,t} = \text{OC}^{\text{vom}}_{i,v,r} + \sum_{f}(\text{FC}_{i,f} \cdot \text{HR}_{i,v,f,r} \cdot (\text{FT}_{f,t} + \text{FR}_{f,r})) \\ + \text{EM}_{i,v,r} \cdot \text{PC}_t \qquad \forall i \in \mathcal{I}, v \in \mathcal{V}, r \in \mathcal{R}, t \in \mathcal{T} \end{aligned} \tag{11}$$

Moreover, firms incur fixed O&M costs from holding generation capacity, costs characterized by the product of $gc_{i,v,r,t}$ and the fixed O&M costs $\text{OC}^{\text{fom}}_{i,r}$ (Equation (12)):

$$c^{\text{fom}}_{r,t} = \sum_{i,v} \text{OC}^{\text{fom}}_{i,r} \cdot gc_{i,v,r,t} \qquad r \in \mathcal{R}, \forall t \in \mathcal{T} \tag{12}$$

In analogy, Equation (13) accounts for variable and fixed costs from electricity exchange between regions. With the variable costs $c^{\text{tvo}}_{r,t}$ being the product of the transaction costs from physical flows $\text{OC}^{\text{tvo}}_{r,rr}$, the actual exchange between regions $e_{s,r,rr,t}$, and the number of hours in each load segment H_s. Fixed maintenance costs for transmission

$c^{\text{tfm}}_{r,t}$ are derived from the accumulated transmission capacity $tc_{r,rr,t}$ times the fixed costs for transmission $\text{OC}^{\text{tfm}}_{r,rr,t}$ (Equation (14)):

$$c^{\text{tvo}}_{r,t} = \sum_{s,rr} \text{OC}^{\text{tvo}}_{r,rr} \cdot e_{s,r,rr,t} \cdot \text{H}_s \qquad \forall r \in \mathcal{R}, t \in \mathcal{T} \tag{13}$$

$$c^{\text{tfm}}_{r,t} = \sum_{rr} \text{OC}^{\text{tfm}}_{r,rr,t} \cdot tc_{r,rr,t} \qquad \forall r \in \mathcal{R}, t \in \mathcal{T} \tag{14}$$

Dispatch

The main equilibrium constraint of a power market is to meet demand at any point in time. Accordingly, the market clearing condition (Equation (15)) requires that generation $g_{s,i,v,r,t}$, plus electricity imports $e_{s,rr,r,t}$, less electricity exports $e_{s,r,rr,t}$, less electricity netexports to outside regions $\text{E}^{\text{int}}_{s,r}$, plus storage discharge $sd_{s,j,r,t}$, less storage charge $s_{s,j,r,t}$, and less self-consumption of hydro pump storage $\text{PS}_{s,r}$ has to meet demand $\text{D}_{s,r,t}$. Moreover, flat loss factors are applied to account for losses from storage discharge ϵ and intra-regional distribution δ.[19] However, a region-specific loss factor is used for exchange between regions with $\text{PEN}^{\text{tr}}_{r,rr}$ being again a function of the distance between the regions' load centers:[20]

$$\begin{aligned}
&(\sum_{i,v} g_{s,i,v,r,t} + \sum_{rr} e_{s,rr,r,t} - \sum_{rr} e_{s,r,rr,t} \cdot \text{PEN}^{\text{tr}}_{r,rr} \\
&- \text{E}^{\text{int}}_{s,r} + \sum_{j} (sd_{s,j,r,t} - s_{s,j,r,t} \cdot (1-\epsilon)) \\
&- \text{PS}_{s,r}) \cdot \text{H}_s \\
&= \text{D}_{s,r,t} \cdot \text{H}_s * (1+\delta) \qquad \forall s \in \mathcal{S}, r \in \mathcal{R}, t \in \mathcal{T}
\end{aligned} \tag{15}$$

To account for physical constraints, generation of controllable generation units $g_{s,i,v,r,t}$, that are comprised in the set $\mathcal{I}_{\text{ctr}}$, is limited by the installed capacity $gc_{i,v,r,t}$.[21] The latter is again constrained by an availability factor for each load segment $\text{AF}_{s,i,r}$ (representing monthly availability patterns of dispatchable generation technologies) or a capacity factor $\text{CF}_{s,i,r}$ for intermittent generation technologies (Equation (16)):

$$g_{s,i,v,r,t} \leq gc_{i,v,r,t} \cdot \text{AF}_{s,i,r} \cdot \text{CF}_{s,i,r} \qquad \forall s \in \mathcal{S}, i \in \mathcal{I}_{\text{ctr}}, v \in \mathcal{V}, r \in \mathcal{R}, t \in \mathcal{T} \tag{16}$$

[19] Note that the storage loss factor ϵ is applied only to the storage charge and consequently captures the losses occurring in the whole storage cycle.

[20] Note that the transmission loss factor $\text{PEN}^{\text{tr}}_{r,rr}$ is applied only to exports and hence captures the losses that occur in the exporting as well as the importing region.

[21] Note that the set of controllable generation units also comprises RES. However, the set excludes generation technologies that operate in multiple energy sectors such as combined heat and power (CHP) power plants.

To approximate observed generation patterns, we define certain must-run capacity by fixing generation at the average capacity factor for the set of non-dispatched generation technologies $\mathcal{I}_{\text{fix}}$, that comprises, for example, geothermal power plants (Equation (17)):

$$g_{s,i,v,r,t} = gc_{i,v,r,t} \cdot \text{AF}_{s,i,r} \cdot \text{CF}_{s,i,r} \qquad \forall s \in \mathcal{S}, i \in \mathcal{I}_{\text{fix}}, v \in \mathcal{V}, r \in \mathcal{R}, t \in \mathcal{T} \tag{17}$$

With the same rationale we apply a lower bound to generation from nuclear power in Equation (18). We set the minimum nuclear generation to the dispatch factor DF_s of its available generation capacity:

$$g_{s,i,v,r,t} \geq gc_{i,v,r,t} \cdot \text{AF}_{s,i,r} \cdot \text{DF}_s \qquad \forall s \in \mathcal{S}, i \in \{nuclear\}, v \in \mathcal{V}, r \in \mathcal{R}, t \in \mathcal{T} \tag{18}$$

Finally, we define, for notification purposes, total generation over all load segments in Equation (19) as

$$tg_{i,v,r,t} = \sum_{s} g_{s,i,v,r,t} \cdot \text{H}_s \qquad \forall i \in \mathcal{I}, v \in \mathcal{V}, r \in \mathcal{R}, t \in \mathcal{T}. \tag{19}$$

Generation capacity

With respect to the development of generation capacity over time, its accumulated capacity $gc_{i,r,t}$ is determined in Equation (20) as the sum of new generation capacity $gc^{\text{new}}_{i,r,t}$ in a specific period and the existing endowment in the previous period $gc_{i,v,r,t-1}$:

$$gc_{i,v,r,t} = gc^{\text{new}}_{i,r,t} + gc_{i,v,r,t-1} \qquad \forall i \in \mathcal{I}_{\text{new}}, v \in \mathcal{V}_{\text{new}}, r \in \mathcal{R}, t \in \mathcal{T} \tag{20}$$

There are upper bounds to investment into new vintage technologies. A limit can be set to each region $\text{CAP}^{\text{gc}}_{i,r,t}$ and an additional one $\text{CAP}^{\text{geu}}_{i,t}$ to the system-wide investment in each technology, which approximates technical limits from the market for generation technologies (Equations (21) and (22)):

$$gc^{\text{new}}_{i,r,t} \leq \text{CAP}^{\text{gc}}_{i,r,t} \qquad \forall i \in \mathcal{I}_{\text{new}}, r \in \mathcal{R}, t \in \mathcal{T} \tag{21}$$

$$\sum_{r} gc^{\text{new}}_{i,r,t} \leq \text{CAP}^{\text{geu}}_{i,t} \qquad \forall i \in \mathcal{I}_{\text{new}}, t \in \mathcal{T} \tag{22}$$

Retirement of generation capacity by firms is endogenous to the EU-REGEN model. New generation capacity has to be retired before its expected lifetime $\text{L}_{i,v,r,t}$, which is a binary variable with a positive number for each period before the time period of retirement at the latest (Equation (23)):

$$gc_{i,v,r,t} \leq gc^{\text{new}}_{i,r,t} \cdot \text{L}_{i,v,r,t} \qquad \forall i \in \mathcal{I}_{\text{new}}, v \in \mathcal{V}_{\text{new}}, r \in \mathcal{R}, t \in \mathcal{T} \tag{23}$$

For existing capacity, in addition to retirement, there is the option of conversion and retrofits, which means allowing for the use of different fuels (e.g., biomass instead of coal) or the addition of a carbon capture facility to, for example, a coal power plant, respectively. We set upper bounds to conventional capacity that can be retrofitted (Equation (24)). Here, the amount of retrofitted capacity, which is determined by $gc_{i,v,r,t}$ and the retrofit factor RF_i, representing the capacity added through the retrofit, has to be below the capacity limit $\mathrm{CAP}^{\mathrm{ret}}_{i,r}$ (approximating technical limits) for the set of possible retrofit technologies $\mathcal{I}_{\mathrm{ret}}$:

$$gc_{i,v,r,t} \cdot \mathrm{RF}_i < \mathrm{CAP}^{\mathrm{ret}}_{i,r} \qquad \forall i \in \mathcal{I}_{\mathrm{ret}}, v \in \mathcal{V}, r \in \mathcal{R}, t \in \mathcal{T} \tag{24}$$

With respect to conversions, existing coal or lignite capacity can be used in conventional mode or converted to using different fuels. Hence, for the retirement of old capacity $gc_{i,v,r,t}$,[22] the sum of old and converted capacity, which is scaled by the conversion factor CR_i (again representing the capacity added through the conversion), cannot exceed the amount of capacity that can still be operated based on the technical lifetime constraint(Equation (25)):

$$gc_{i,v,r,t} + \sum_{i \in \mathcal{I}_{\mathrm{cr}}} gc_{i,v,r,t} \cdot \mathrm{CR}_i \leq \mathrm{GC}^{\mathrm{old}}_{i,v,r} \cdot \mathrm{L}_{i,v,r,t} \qquad \forall i \in \mathcal{I}_{\mathrm{cr}}, v \in \mathcal{V}_{\mathrm{old}}, r \in \mathcal{R}, t \in \mathcal{T} \tag{25}$$

Finally, as indicated in Equation (26), we make sure that generation capacity in each vintage retires monotonically decreasing:

$$gc_{i,v,r,t+1} \leq gc_{i,v,r,t} \qquad \forall i \in \mathcal{I}, v \in \mathcal{V}, r \in \mathcal{R}, t \in \mathcal{T} \tag{26}$$

Storage

The operation of electricity storage is constrained by the available storage and charge capacity. The former is determined by the sum of new capacity $sc^{\mathrm{new}}_{j,r,t}$ and existing capacity from the previous period $sc_{j,r,t-1}$ (Equation (27)):

$$sc_{s,r,t} = sc^{\mathrm{new}}_{j,r,t} + sc_{j,r,t-1} \qquad \forall j \in \mathcal{J}, r \in \mathcal{R}, t \in \mathcal{T} \tag{27}$$

This charge capacity $sc_{j,r,t}$ is then the upper limit to the dispatch of storage charge $s_{s,j,r,t}$ and discharge $sd_{s,j,r,t}$, as depicted in Equations (28) and (29):

$$s_{s,j,r,t} \leq sc_{j,r,t} \qquad \forall s \in \mathcal{S}, j \in \mathcal{J}, r \in \mathcal{R}, t \in \mathcal{T} \tag{28}$$

[22] The parameter $gc_{i,v,r,t}$ captures all units operated in the base year.

$$sd_{s,j,r,t} \leq sc_{j,r,t} \qquad \forall s \in \mathcal{S}, j \in \mathcal{J}, r \in \mathcal{R}, t \in \mathcal{T} \tag{29}$$

Furthermore, Equation (30) limits the accumulated amount of stored electricity $sb_{s,j,r,t}$ to the storage capacity, which is determined by a fixed size SH_j (≥ 1) in relation to the charge capacity $sc_{j,r,t}$:

$$sb_{s,j,r,t} \leq \mathrm{SH}_j \cdot sc_{j,r,t} \qquad \forall s \in \mathcal{S}, j \in \mathcal{J}, r \in \mathcal{R}, t \in \mathcal{T} \tag{30}$$

The dynamic accumulation of $sb_{s,j,r,t}$ is defined in Equation (31) as the amount of stored electricity in the previous time segment $sb_{s-1,j,r,t}$ plus the net charge, which is the difference between the storage charge $s_{s,j,r,t}$ and the storage discharge $sd_{s,j,r,t}$:

$$sb_{s,j,r,t} \leq sb_{s-1,j,r,t} + H_s \cdot (s_{s,j,r,t} - sd_{s,j,r,t}) \qquad \forall s \in \mathcal{S}, j \in \mathcal{J}, r \in \mathcal{R}, t \in \mathcal{T} \tag{31}$$

Transmission

As introduced in Section 2, the representation of electricity transmission in the EU-REGEN model is limited to exchange between regions. Its available capacity is the sum of new transmission capacity $tc^{\mathrm{new}}_{i,r,t}$ and the capacity in the previous period $gc_{i,r,t-1}$ as shown in Equation (32):

$$tc_{r,rr,t} = tc^{\mathrm{new}}_{r,rr,t} + tc_{r,rr,t-1} \qquad \forall r \in \mathcal{R}, t \in \mathcal{T} \tag{32}$$

To account for the political and technical feasibility of additions to transmission capacity, we set upper limits to it. For each time period, bounds can be applied to each individual connection between regions $\mathrm{CAP}^{\mathrm{tc}}_{r,rr,t}$ (Equation (33)) as well as to system-wide additions $\mathrm{CAP}^{\mathrm{teu}}_{t}$ in a specific time period (Equation (33)):

$$tc^{new}_{r,rr,t} < \mathrm{CAP}^{\mathrm{tc}}_{r,rr,t} \qquad \forall r \in \mathcal{R}, t \in \mathcal{T} \tag{33}$$

$$\sum_{r} tc^{new}_{r,rr,t} \cdot \mathrm{TL}_{r,rr} < \mathrm{CAP}^{\mathrm{teu}}_{t} \qquad \forall t \in \mathcal{T} \tag{34}$$

Geologic storage of carbon

The EU-REGEN framework allows for the geologic storage of CO_2 captured from electricity generation facilities.[23] For that purpose, the physical accumulation of the stored CO_2 is determined, as shown in Equation (35), by the product of capture rate CR_i, fuel coefficient FC_i, heat rate $\mathrm{HR}_{i,f,r}$, fuel-specific carbon content CC_f, and generation

[23] Note that we only consider the storage of CO_2 and abstract from the depiction of the CO_2 transportation infrastructure.

$tg_{i,v,r,t}$

$$cs_{r,t} = \sum_{i,v,f} \mathrm{CR}_i \cdot \mathrm{FC}_i \cdot \mathrm{HR}_{i,f,r} \cdot \mathrm{CC}_f \cdot tg_{i,v,r,t} \qquad \forall r \in \mathcal{R}, t \in \mathcal{T} \tag{35}$$

with its dynamic accumulation being constrained in Equation (36) by the geological storage capacity $\mathrm{CAP}^{\mathrm{ccs}}_r$:

$$\sum_r cs_{r,t} < \mathrm{CAP}^{\mathrm{ccs}}_r \qquad \forall r \in \mathcal{R} \tag{36}$$

Resource constraints

Furthermore, the dispatch and investment of generation technologies is limited by the availability of resources. With respect to wind and solar technologies, the limited availability of land area as well as competition with alternative land use types leads to limited potential within each resource class (see Section 5). As shown in Equations (37) and (38), for both groups of technologies, accumulated capacity additions and initial capacity $gc_{i,v,r,t}$ in each quality class, with $\mathrm{QC}_{i,r}$ allocating existing capacities to quality classes, must not exceed the capacity limits $\mathrm{CAP}^{\mathrm{wind}}_{i,r}$ and $\mathrm{CAP}^{\mathrm{solar}}_{i,r}$ (see Section 7):

$$\sum_v gc_{i,v,r,t} + \mathrm{QC}_{i,r} \cdot \sum_{v \in \mathcal{V}_{\mathrm{old}}} gc_{i,v,r,t} < \mathrm{CAP}^{\mathrm{wind}}_{i,r} \qquad \forall i \in \mathcal{I}_{\mathrm{wind}}, r \in \mathcal{R}, t \in \mathcal{T} \tag{37}$$

$$\sum_v gc_{i,v,r,t} + \mathrm{QC}_{i,r} \cdot \sum_{v \in \mathcal{V}_{\mathrm{old}}} gc_{i,v,r,t} < \mathrm{CAP}^{\mathrm{solar}}_{i,r} \qquad \forall i \in \mathcal{I}_{\mathrm{solar}}, r \in \mathcal{R}, t \in \mathcal{T} \tag{38}$$

Concerning biomass and gas, their availability is bounded by regional supply. As depicted in Equation (39), regional exogenous biomass supply $\mathrm{BS}_{b,r,t}$ is differentiated between supply classes b, which constrain biomass fuel use that is determined by the fuel use coefficient $\mathrm{FC}_{i,f}$, heat rate $\mathrm{HR}_{i,f,r}$, and annual generation $tg_{i,v,r,t}$ (see also Section 7):

$$\sum_b \mathrm{BS}_{b,r,t} \geq \sum_{i,v} \sum_{f \in \{bio\}} \mathrm{FC}_{i,f} \cdot HR_{i,f,r} \cdot tg_{i,v,r,t} \qquad \forall r \in \mathcal{R}, t \in \mathcal{T} \tag{39}$$

By analogy, gas demand is constrained in Equation (40) by exogenous gas supply $\mathrm{GS}_{g,r,t}$ over all gas supply classes g:

$$\sum_g \mathrm{GS}_{g,r,t} \geq \sum_{i,v} \sum_{f \in \{gas\}} \mathrm{FC}_{i,f} \cdot \mathrm{HR}_{i,f,r} \cdot tg_{i,v,r,t} \qquad \forall r \in \mathcal{R}, t \in \mathcal{T} \tag{40}$$

The CO_2 permit market

As outlined in Section 2, the EU-REGEN framework addresses the environmental externality from fuel combustion by limiting the total amount of emissions and thus includes

a market for CO_2 emissions from electricity generation.[24] In the default setting, the market for CO_2 permits does not allow for banking, that is, CO_2 emissions have to be offset in the period of occurrence. In that case, the amount of net banked credits nbc_t is set to zero. Meaning, in each period the amount of emitted carbon, which is characterized by the emission rate $\mathrm{EM}_{i,r}$ and total generation $tg_{i,v,r,t}$, cannot be above the CO_2 emission cap $\mathrm{CAP}_t^{\mathrm{co2}}$ (Equation (41)):[25]

$$\mathrm{CAP}_t^{\mathrm{co2}} - nbc_t \geq \sum_{i,v,r} \mathrm{EM}_{i,r} \cdot tg_{i,v,r,t} \qquad t \in \mathcal{T} \tag{41}$$

However, banking of permits can be allowed by introducing a banking market. Then, the banking market is modeled by the cumulative banked credits cbc_t, through the arithmetic series indicated in Equation (42),

$$cbc_t = \sum_{t'<t} nbc_{t'} \qquad \forall t \in \mathcal{T} \tag{42}$$

including the constraint that accumulated banked credits balance by the model horizon (Equation (43)):

$$\sum_{t<2050} nbc_t = 0 \tag{43}$$

[24] Note that the model as well allows for introducing a carbon tax or exogenous carbon permit price (see Equation (11)).

[25] The magnitude of the CO_2 cap depends on the scenario of interest.

4. Model resolution

Spatial

The EU-REGEN model represents the European power market. Its geographic scope includes all countries of the European Union (EU28), except for the island countries Malta and Cyprus. Additionally, the model includes Switzerland and Norway, which have a central position in the European system or are endowed with great resource potentials. To reduce the size of the model, those 28 countries are grouped into 13 model regions.[26] The aggregation is based on geographic characteristics and current configurations of the European power markets. However, Germany is disaggregated into a northern and southern region to reflect existing transmission limitations between the two regions—which triggered the current public debate on two pricing zones within Germany (e.g., Egerer et al., 2015, 2016). Figure 3 shows the EU-REGEN model regions.

Figure 3: EU-REGEN model regions and transmission links in the base year

[26] See Table B.8 in Appendix Appendix B for an overview of the composition of model regions.

Temporal

The model horizon in the default model setting is 2050. We start with the base year 2015 (with given capacity) and optimize dispatch and investment in 5-year time steps up to 2050, which amounts to eight steps. Simulating dispatch on an hourly basis, or an even higher temporal resolution, offers the most accurate representation of power system operation. Yet, similar to the spatial aggregation described above, the number of time segments is reduced within each period for computational reasons. The default version of the model uses 121 intra-annual time segments. More information on the choice of representative hours can be found in Section 6. However, this reduced form approach means loss of the chronological order of hours and, thereby, compromises the modeling quality of, for example, electricity storage. Thus, electricity storage is only considered when looking at a single time period, where an hourly resolution is again feasible.

Technology

The model includes 25 different types of generation capacity (see Table B.9 in Appendix Appendix B). To account for different characteristics of power plants of the same type or varying resource quality of variable RES, each type is further distinguished into generation blocks. This results in 73 different generation blocks by region with, for example, wind power making up for six blocks due to six different wind resource classes (see Section 5). Moreover, existing generation units are grouped into vintages to allow for different heat rates among generation blocks. Each vintage covers a period of five years and includes all units that went online in this period. New capacity can be added to each technology block through investment. Similar to existing installations, additions in different model periods are grouped into vintages to assign specific technological characteristics to each. As depicted in Section 3, generation capacity can be subject to upper bounds on additions or on accumulated capacity. Limits on additions are applied to nuclear power and accumulated capacity of each variable RES technology. Finally, the set of non-dispatchable technologies comprises geothermal and combined heat and power (CHP), and the set of technologies eligible for retrofit or conversion consists of hard coal, lignite, and gas power.

With respect to CCS, there is no commercially operated power plant in Europe as of now (EC, 2013b). In the model, new CCS generation technology can be added in combination with new generation capacity for lignite, coal, natural gas, or biomass power. Retrofits of existing conventional generation capacity is as well enabled for lignite, coal, and biomass power plants. Furthermore, the amount of captured CO_2 is subject to limited geological storage capacity.

As indicated in Section 3, we abstract from intra-regional electricity distribution and model electricity exchange between regions only. We assume one generic type of transmission technology, whose investment costs, however, vary among regions to account for, for example, oversees connections. Existing transmission capacities between regions serve as starting values. In each time period, new transmission capacity can be added between neighboring regions or regions with an already existing transmission link. However, those additions are subject to upper bounds.

5. Modeling wind and solar technologies

The importance of a detailed representation of the intermittency of RES has been emphasized in, for example, Joskow (2011). The modeling of variable RES has to incorporate both components of the market value (see Section 2), the energy value and the demand matching capability (Lamont, 2008). Yet, so far, little effort has been put into methodologies to capture the temporal, inter-regional, and intra-regional variations in a dynamic investment model. Our modeling approach accounts, on the one hand, for varying annual electricity generation from variable RES between and within regions. On the other hand, differences in the temporal profiles are captured. Therefore, the characteristics of the resources, wind speed, and solar irradiation, and their different technologies are captured in our modeling approach. In the following, we will outline the methodology for the detailed representation of variable RES in the EU-REGEN framework.

5.1. Resource data base

To fully account for the intermittency and spatial variability of resources, the underlying data on wind and solar resources is required to be at a high temporal and spatial resolution. Similar to other studies (e.g., Cannon et al., 2015; Juruš et al., 2013; Olauson and Bergkvist, 2015), we use the MERRA (Modern-Era Retrospective analysis for Research and Applications) reanalysis data for both resources, which is provided by NASA (Rienecker et al., 2011). Parameters are available for the time interval between 1979 and today with a temporal resolution of 1 hour. The spatial resolution is $\frac{1}{2}$ and $\frac{1}{3}$ degree in latitude and longitude, respectively. Meaning, EU REGEN's geographic scope is covered by 2,704 locations, each one representing an area of $\frac{1}{2} \times \frac{1}{3}$ degree. Figure 4a illustrates the spatial resolution of the MERRA data set with different colors representing each model region and gray-colored grid cells indicating offshore area. For wind resources, we extract variables on eastward and northward wind speed at 50 meters above the surface (U50M and V50M), displacement height (DISPH), and roughness length (Z0M). Modeling solar power technologies is based on MERRA's surface incident shortwave flux (SWGDN) and the temperature 2 meters above displacement height (T2M) (NASA, 2010):

5.2. Resource classes

As mentioned above, the EU-REGEN model captures the varying quality of variable RES through different generation blocks. The generation blocks of new variable RES vintages represent the different resource classes for each resource type. Concerning wind, we introduce six resource classes C_{wind} based on the wind speed at 100 m above ground. Classes are defined as shown in Table 1:

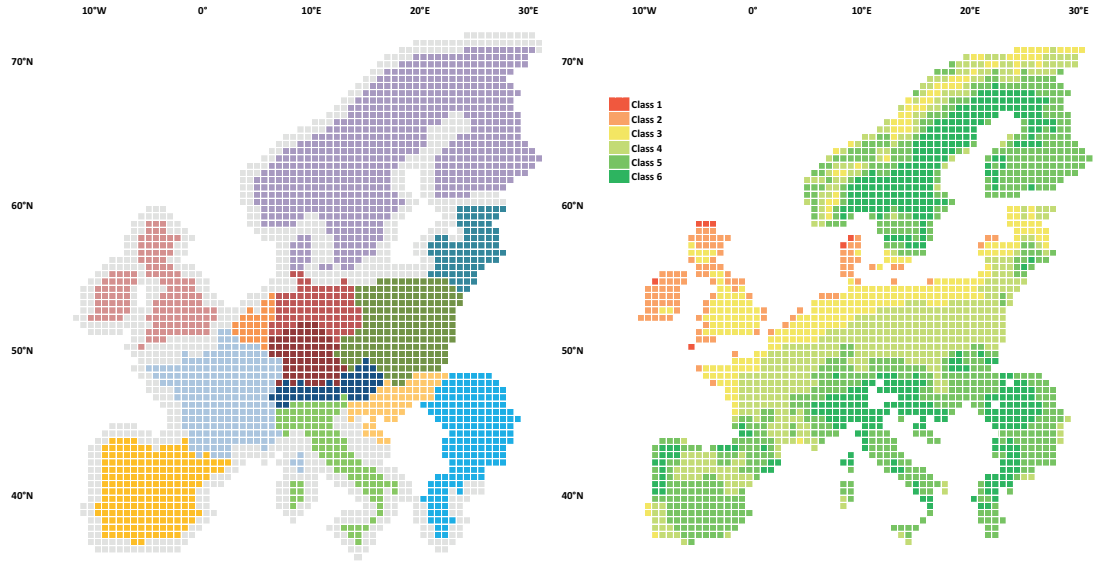

(a) Resolution

(b) Distribution of wind resource classes

Figure 4: Wind resource data base

Table 1: Wind resource classes based on average wind speed at 100 m [m/s]

$Wind\ 6$	$Wind\ 5$	$Wind\ 4$	$Wind\ 3$	$Wind\ 2$	$Wind\ 1$
< 4	$4-5$	$5-6$	$6-7$	$7-8$	> 9

To determine the resource quality in each of the 2,704 locations, we calculate the average wind speed over the time period 1982 to 2013. By means of that measure, we allocate each location to one resource class within its region. An overview of the spatial distribution of resource classes is indicated in Figure 4b.

The same approach is applied to solar resources. Here, resource classes C_{solar} are based on the mean global horizontal irradiation from 1982 to 2013 (Table 2). Assigning a solar resource class to each location lead to the distribution shown in Figure C.6a in Appendix Appendix C.

Table 2: Solar resource classes based on average solar irradiation [kWh/m^2]

$Solar\ 6$	$Solar\ 5$	$Solar\ 4$	$Solar\ 3$	$Solar\ 2$	$Solar\ 1$
$< 1{,}000$	$1{,}000-1{,}200$	$1{,}200-1{,}400$	$1{,}400-1{,}600$	$1{,}600-1{,}800$	$> 1{,}800$

Due to its high investment costs, we assume concentrated solar power (CSP) to be suitable only for locations with high resource quality. Therefore, CSP is limited to locations within solar classes 1 and 2, as shown in Figure C.6b in Appendix Appendix C.

5.3. Wind power

In terms of wind power, we consider wind onshore and offshore as separate technologies. As of the end of 2016, 154 GW of cumulative wind power capacity was installed

in the EU. A majority of 141 GW was installed onshore compared to 13 GW of offshore installations (Wind Europe, 2017). Moreover, cost and performance estimates of both technologies differ. Therefore, it is crucial to differentiate between them to capture the technological traits and economics of wind power.

Estimating the generation profile of wind power, which captures the availability of a wind power technology in each time segment, requires data on wind speed, displacement height, and surface roughness. The translation of these three input parameters into power output is based on three steps. First, the combination of wind speeds from two directions. Then, the extrapolation of wind speeds to hub heights. Finally, the translation of wind speeds for combinations of different hub heights and wind turbines to a normalized power output. We provdide a detailed elaboration of these steps in Section Appendix E in Appendix Appendix E. Moreover, the nomenclature of the sets, variables, and parameters used in this section is described in Table D.10 in Appendix Appendix D.

However, the purpose of EU-REGEN requires region-wide profiles for existing and new vintages by resource class and, furthermore, profiles separated into onshore and offshore installations. In the following, we will outline the aggregation of profiles by locations to region-wide profiles for existing and new vintages.

Existing vintages

For existing onshore vintages, we extrapolate wind speeds (see Equation (E.2) in Appendix Appendix E) to a hub height of 100 m and calculate the mean wind speed s_l^{m} over the time period from 1982 to 2013. This is used to assign locations l within each region to different site qualities $Q = \{low, medium, high\}$. Each site quality q is determined by upper limits s_q^{up} and lower limits s_q^{low} (Equation (44)):

$$\mathcal{L}_{\mathrm{q}} = \{(s_l^{\mathrm{m}} \geq s_q^{low}) \vee (s_l^{\mathrm{m}} l s_q^{up})\} \qquad \forall l \in \mathcal{L}_{\mathrm{on}}, q \in \mathcal{Q} \tag{44}$$

Based on that, we calculate a weighted-average of the normalized wind power output $wp_{s,l,h,g}^{\mathrm{trb}}$ in a region over all turbine types and locations $wp_{s,h,q,r}^{\mathrm{hub}}$ (see Appendix Appendix E). This aims at approximating the current average configuration of an installed wind turbine in each region. Hence, we use, on the one hand, weights on the existing capacity distribution among sites within a region $W_{l,r}^{\mathrm{wc}}$. On the other hand, we apply a weighting for the assumed existing technology mix of hub heights and turbines within site qualities in each region $W_{h,g,q,r}^{\mathrm{wt}}$:

$$wp_{s,h,q,r}^{\mathrm{hub}} = \frac{\sum_g \sum_{l \in \mathcal{L}_{\mathrm{on}}} W_{l,r}^{\mathrm{wc}} \cdot W_{h,g,q,r}^{\mathrm{wt}} \cdot wp_{s,l,h,g}^{\mathrm{trb}}}{\sum_g \sum_{l \in \mathcal{L}_{\mathrm{on}}} W_{l,r}^{\mathrm{wc}} \cdot W_{h,g,q,r}^{\mathrm{wt}}} \qquad \forall s \in \mathcal{S}, h \in \mathcal{H}_{\mathrm{ex}}, q \in \mathcal{Q}, r \in \mathcal{R} \tag{45}$$

In a second step, we calculate the weighted average across hub heights and quality classes: ($W^{\text{hub}}_{h,q,r}$ and $W^{\text{q}}_{h,r}$) to get a single region-wide profile (Equation (46)). Furthermore, the turbine output is subject to loss factors σ^u and σ^p_s that represent a general loss and seasonal maintenance factor, respectively. So, we finally arrive at the normalized power output for each region and resource class:

$$wp^{on}_{s,r} = \sigma^u \cdot \sigma^p_s \cdot \frac{\sum_{h,q} W^{\text{q}}_{h,r} \cdot W^{\text{hub}}_{h,q,r} \cdot wp^{\text{hub}}_{s,h,q,r}}{\sum_{h,q} W^{\text{q}}_{h,r} \cdot W^{\text{hub}}_{h,q,r}} \qquad \forall s \in \mathcal{S}, r \in \mathcal{R} \tag{46}$$

We follow an analog approach for offshore applications. However, we abstract from different site qualities:

$$wp^{\text{hub-os}}_{s,h,r} = \frac{\sum_g \sum_{l \in \mathcal{L}_{\text{os}}} W^{\text{wc}}_{l,r} \cdot W^{\text{wto}}_{h,g,r} \cdot wp^{\text{trb}}_{s,l,h,g}}{\sum_g \sum_{l \in \mathcal{L}_{\text{os}}} W^{\text{wc}}_{l,r} \cdot W^{\text{wto}}_{h,g,r}} \qquad \forall s \in \mathcal{S}, h \in \mathcal{H}_{\text{ex}}, r \in \mathcal{R} \tag{47}$$

$$wp^{os}_{s,r} = \sigma^u \cdot \sigma^p_s \cdot \frac{\sum_h W^{\text{hub-os}}_{h,r} \cdot wp^{\text{hub}}_{s,h,r}}{\sum_h W^{\text{hub-os}}_{h,r}} \qquad \forall s \in \mathcal{S}, r \in \mathcal{R} \tag{48}$$

New vintages

Concerning new onshore and offshore vintages, we aggregate the output $wp^{\text{trb}}_{s,l,h,g}$ for each location to a single profile comprising all locations within each quality class C_{wind} in a region. The binary parameter $C^{\text{wind}}_{r,l,c}$ allocates each location to its resource class as depicted in Equation (49):

$$wp^{reg}_{s,r,c,h,g} = \frac{\sum_l wp^{\text{trb}}_{s,l,h,g} \cdot C^{wind}_{r,l,c}}{\sum_l C^{wind}_{r,l,c}} \qquad \forall s \in \mathcal{S}, r \in \mathcal{R}, c \in \mathcal{C}_{\text{wind}}, h \in \mathcal{H}_{\text{new}}, g \in \mathcal{G} \tag{49}$$

The final profile by region, quality class, and vintage is calculated by assuming a specific combination of hub-height and turbine type to each vintage year $W^{wind}_{r,h,g,v}$ (Equation (50)). We apply this approach to approximate technological progress. In analogy to existing installations, the loss factors σ^u and σ^p_s apply:

$$wp_{s,r,c} = \sigma^u \cdot \sigma^p_s \cdot \frac{\sum_{h,g} wp^{reg}_{s,r,c,h,g} \cdot W^{wind}_{r,h,g,v}}{\sum_{h,g} W^{wind}_{r,h,g,v}} \qquad \forall s \in \mathcal{S}, r \in \mathcal{R}, c \in \mathcal{C}_{\text{wind}} \tag{50}$$

Note that values of $wp_{s,r,c}$ directly yield into the capacity factor $\text{CF}_{s,i,r}$ introduced in Equation (16) in Section 3. Moreover, we approximate values for the parameters σ^u, σ^p_s, $W^{\text{hub-os}}_{h,r}$, $W^{\text{wc}}_{l,r}$, and $W^{\text{tec-os}}_{h,g,r}$ from the model calibration.

5.4. Solar power

With respect to solar power, we differentiate between three different types of solar power technologies: stationary photovoltaic (PV), tracking photovoltaic (PV-TK), and

CSP. Currently, only PV is widely applied in Europe with 100 GW of installed capacity in 2016 (Eurostat, 2018). Yet, especially a long-term model on decarbonization paths, which is driven by the economics of generation technologies, should incorporate a great variety of solar power technologies. On the one hand, this allows for analyzing the impact of different relative costs among solar power technologies. On the other hand, PV, PV-TK, and CSP differ in their output profiles. This is due to the higher flexibility of PV-TK and CSP in terms of tracking and storage, respectively (Huld et al., 2008).

We can estimate generation profiles for solar power technologies by using direct and diffuse irradiance and ground temperature as input parameters. For all three technologies, the two main components of solar irradiation, direct and diffuse radiation flux, affect the output differently. Yet, solar irradiation data on a high spatial and temporal resolution is only reported for global horizontal irradiation (GHI). Hence, we have to separate the GHI into its direct and diffuse components before being able to estimate the power output. The methodology for separating solar irradiation in its components is explained in Appendix Appendix G. Moreover, the nomenclature of the sets, variables, and parameters used in this section is described in Table F.11 in Appendix Appendix F.

The conversion of the two components of solar irradiation and temperature to normalized output requires four main steps. We start by calculating the hourly angle of the sun's rays. This allows, in a second step, for calculating the overall solar irradiation at the module. Then, this has to be corrected for the panel efficiency and in a final step for the inverter efficiency. These steps result in the normalized solar power feed-in profile $sp_{s,l,o,p}$ by location and for different orientations o and tilts p. We provide a detailed description of these steps in Appendix Appendix H. In analogy to wind power, we derive different profiles for varying vintages and technologies of solar power in the following.

Existing vintages

In a first step, profiles for existing PV installations are approximated in Equation (51) by weight $W^{\text{sc}}_{l,r}$ for the existing capacity distribution among locations within a region on the normalized solar power output $sp_{s,l,o,p}$:[27]

$$sp^{reg}_{s,r,o,p} = \frac{\sum_l sp_{s,l,o,p} \cdot W^{\text{sc}}_{l,r}}{\sum_l W^{\text{sc}}_{l,r}} \qquad \forall s \in \mathcal{S}, r \in \mathcal{R}, o \in \mathcal{O}, p \in \mathcal{P} \tag{51}$$

[27] Note that we assume existing PV installations to be stationary only.

Thereafter, we apply a distribution $W^{\text{st}}_{o,p}$ for combinations of orientation and panel tilt to get a single profile by region (Equation (52)):

$$sp^{pv}_{s,r} = \frac{\sum_{o,p} sp^{reg}_{s,r,o,p} \cdot W^{\text{st}}_{o,p}}{\sum_{o,p} W^{\text{st}}_{o,p}} \qquad \forall s \in \mathcal{S}, r \in \mathcal{R} \tag{52}$$

New vintages

For new static PV vintages, we assume a south-facing module with an optimal panel tilt based on Masters (2004). We aggregate the normalized solar power output $sp_{s,l,o,p}$ from Equation (H.11) in Appendix Appendix H for each location to a single profile comprising all locations within quality classes C_{solar} and for each region as depicted in Equation (53). The binary parameter $C^{\text{solar}}_{r,l,c}$ allocates each location to its resource class:

$$sp^{pv}_{s,i,r} = \frac{\sum_{o \in \{south\}} \sum_{p \in \{opt\}} \sum_{l} sp_{s,l,o,p} \cdot C^{solar}_{r,l,c}}{\sum_{l} C^{solar}_{l,c}} \qquad \forall s \in \mathcal{S}, i \in \{pv\}, r \in \mathcal{R} \tag{53}$$

New vintages of tracking PV are supposed to be single-axis, horizontally tracking systems with optimal tilting.[28] Thus, the output profile being calculated by

$$sp^{pv}_{s,i,r} = \frac{\sum_{p \in \{opt\}} \sum_{l} sp_{s,l,o,p} \cdot C^{solar}_{r,l,c}}{\sum_{l} C^{solar}_{l,c}} \qquad \forall s \in \mathcal{S}, i \in \{pvtk\}, r \in \mathcal{R}. \tag{54}$$

Again, $sp^{pv}_{s,r}$, $sp^{npv}_{s,i,r}$, $sp^{ntk}_{s,i,r}$ directly yields into the capacity factor $\text{CF}_{s,i,r}$ of the model framework and values for $W^{\text{sc}}_{l,r}$, $W^{\text{st}}_{o,p}$, and $C^{solar}_{r,l,c}$ are derived from model calibration results.

Model for CSP power generation

In contrast to PV technologies, CSP utilizes only direct normal irradiation $dni_{s,l}$ and includes a storage system. Due to the latter point, besides incoming radiation, the operation of a CSP system is influenced by electricity prices. For that purpose, we simulate the optimal dispatch of CSP based on prices from a static model run of the base year 2015 and derive a generation profile from that optimization exercise, as done in Young et al. (2013). Moreover, the nomenclature of the sets, variables, and parameters used in this paragraph is described in Table I.12 in Appendix Appendix I.

We define the objective function (Equation (55)) as the revenue rev from CSP dispatch $g_{s,i,r}$ at prices $P_{s,r}$:

$$rev = \sum_{s,i,r} g_{s,i,r} \cdot P_{s,r} \tag{55}$$

[28] Note that this means that the modules orientation α^2_o constantly equals the sun's azimuth angle $\alpha^1_{s,l}$ with Equation (H.2) in Appendix Appendix H resolving to $\theta_{s,l,p} = \sin(\beta^1_{s,l}) \cdot \cos(\beta^2_{l,p})$.

Dispatch is constrained by the incoming irradiation $dni_{s,i,r}$, CSP storage charge $s^{csp}_{s,i,r}$, and discharge $sd^{csp}_{s,i,r}$ (Equation (56)) with the solar multiple SM being the relative size of the solar capacity to the CSP turbine capacity:

$$g_{s,i,r} \leq SM \cdot dni_{s,i,r} + sd^{csp}_{s,i,r} - s^{csp}_{s,i,r} \qquad \forall s \in \mathcal{S}, i \in \mathcal{I}_{\text{csp}}, r \in \mathcal{R} \tag{56}$$

Furthermore, the amount of stored electricity $sb^{csp}_{s,i,r}$ is limited by the storage capacity SH^{csp} in hours of turbine capacity (Equation (57))

$$sb^{csp}_{s,i,r} < SH^{csp} \qquad \forall s \in \mathcal{S}, i \in \mathcal{I}_{\text{csp}}, r \in \mathcal{R} \tag{57}$$

and its dynamic accumulation is defined as in Equation (58):

$$sb^{csp}_{s,i,r} = (1 - \epsilon^{csp}) \cdot sb^{csp}_{s-1,i,r} + s^{csp}_{s,i,r} - sd^{csp}_{s,i,r} \qquad \forall s \in \mathcal{S}, i \in \mathcal{I}_{\text{csp}}, r \in \mathcal{R} \tag{58}$$

We assume a storage loss of $\epsilon^{csp} = 0.05$, a solar multiple of $SM = 2.5$, and a storage capacity of $SH^{csp} = 6$ (Young et al., 2013).

6. Aggregation of time segments

Due to computational limitations, it is not feasible to run a dynamic dispatch and investment model with all 8,760 hours in each time period. Therefore, the number of time segments has to be reduced from 8,760 to a couple of hundred by choosing a subset of hours and weighting those. For that purpose we use a two-stage methodology developed for the US-REGEN model.[29]

First, the choice of representative hours is based on identifying the extreme values of the three dimensions per model region: normalized hourly electricity demand, wind, and solar feed-in.[30] We identify the extreme values in all possible one-dimensional, two-dimensional, and three-dimensional spaces of wind, solar, and load. This means, for the one-dimensional spaces, we select the hours with minimum and maximum wind, solar, and load values (6 per region). With respect to the two-dimensional spaces, we select hours representing the vertices of all possible two-dimensional combinations of wind, solar, and load (12 per region). Finally, we select the eight vertices of the three-dimensional wind, solar, and load space (8 per region). With respect to the 16 regions used for the identification of representative hours, this would result in $26 \cdot 16 = 416$ extreme hours. However, some representative hours are an extreme in multiple regions, which reduces the number of hours already to 211. Furthermore, the algorithm is designed in such a way that it does not have to pick the hour with the most extreme values. Instead, it sets this particular hour as the vertex (in the three-dimensional space) and allows for choosing an hour that has a certain distance from the vertex. This allows us to reduce the number of required time segments to 121 when allowing for a distance of 1%.

Second, a weighting of representative hours is crucial to maintain the distribution of the hourly demand, wind, and solar profiles. Weights for each segment are chosen to minimize the sum of squared errors between the aggregated averages and the hourly averages across model regions for demand, wind, and solar profiles (Young et al., 2013).

[29] See Blanford et al. (2018) for detailed information.

[30] We include an additional region for each of the model regions Britain, Iberia, and Scandinavia. For Iberia, we further include the existing feed-in from CSP. Concerning Britain and Iberia, we consider feed-in profils for future wind installations as well. Hence, we end up with 16 regions for the choice of representative hours.

7. Input data

Section 5 depicted how the input parameters for wind and solar power availability are derived. In the following, we provide an overview of the values of other main input parameters.

Generation technologies

As mentioned in Section 4, we differentiate between 25 general types of generation technologies (Table B.9 in Appendix Appendix B). We use the UDI World Electric Power Plants Data Base (Platts, 2013) to compile an inventory of each existing generation technology by vintage for each region. Estimates for heat rate by technology and vintage are based on model calibration and observed values. For the annual discount rate and investment tax rate, the model assumes rates of 7% and 30%, respectively. Availability factors for dispatchable generation technologies are derived from observed seasonal generation patterns (Eurostat, 2014) and the model calibration for the year 2012, which was chosen due to data availability reasons.

The assumed lifetime is based on assumptions in IEA (2013) and holds for existing vintages as well as capacity additions within the model horizon. The same holds true for flat variable and fixed O&M cost with values taken from Schröder et al. (2013) (see Table J.13 in Appendix Appendix J for both).

Assumptions on investment cost for vintages of new generation capacity (Table J.14 in Appendix Appendix J) are based on Schröder et al. (2013). We assume flat cost curves for most conventional generation technologies. Costs for new RES and CCS capacity decrease over time, assuming cost reductions through learning and economies of scale (Table J.14 Appendix Appendix J). The costs for tracking photovoltaic installations are derived from those of static photovoltaic by adding a 25% mark-up.

Concerning investment into dispatchable generation technologies, we set specific public attitudes and capacity limits for nuclear power in each region as a default. In general, capacity additions of nuclear power are not allowed in the following regions in any time period: Benelux, Germany-N, Germany-S, Iberia, Alpine, and Italy. Moreover, based on projected commissioning dates of current units under construction from World Nuclear Association (2014), nuclear power plant capacities of 1.75 GW for France, 1.7 GW for Scandinavia, and 0.94 GW for Eastern Europe-NW are assumed to be complete by 2020. After 2020, capacity additions are unconstrained in regions eligible for nuclear power additions.

Fuel-powered generation technologies in the EU-REGEN model either require lignite, coal, natural gas, oil, or biomass. We apply system-wide and flat fuel prices that are subject to regional adjustment factors (IEA, 2012). For biomass, cost varies for dif-

Table 3: Overview of fuel prices and carbon contents

Fuel type	Fuel price [€/MWh]	Carbon content [tCO2/GJ]
Lignite	3.5	0.099
Coal	14	0.094
Natural gas	33.5	0.056
Oil	64	0.074
Biomass	17 – 36	0.099

ferent biomass supply classes to approximate an upward-sloped supply curve (Section 7). The fuel-specific carbon content and basic fuel prices are indicated in Table 3.

Wind and solar potentials

In addition to the resource class specific time profiles described in Section 5, the detailed representation of variable RES requires data on the capacity potentials in each of those classes, that is, the maximum amount of accumulated capacity. The potential capacity by resource class depends on a variety of factors, for example, exclusion areas, siting constraints, and local topography. Therefore, we use data provided by AWS Truepower (AWS). AWS uses a two-stage approach to provide separate potential values for wind onshore, wind offshore, utility-scale solar, and distributed solar applications. In a first step, an extended geographic-information-system (GIS) analysis is carried out to determine the area that is actually available to the deployment of wind power. This is followed by estimating the capacity of power plants that could be installed in this area by assuming a certain capacity density by area of available land. Values are calculated for each of the above-mentioned applications, resource classes, and model regions. An overview of the sum of capacity potential over resource classes by variable RES and region is presented in Table 4.

Biomass potentials

As indicated above, we approximate the limited supply of biomass for electricity generation with four biomass supply classes. The biomass energy potential for each country and each of these classes is estimated based on numbers from Elbersen et al. (2012). Similar to Bruninx et al. (2015), we group different kinds of biomass to each supply class: ranging from class 1, which comprises cheap and local resources, to class 4 with industrially grown energy crops. Table 5 shows an overview of the composition of biomass supply classes. Moreover, as done in Nahmmacher et al. (2014), we assume 50% of biomass energy potential to be available for the power market.

Demand

We introduced in Section 2 that EU-REGEN's demand side is modeled exogenously. We assume the 2012 hourly electricity demand pattern (ENTSO-E, 2014c) to be valid for

Table 4: Upper limits on variable RES capacities [GW]

Region	Wind-on	Wind-os	PV
Britain	238	74	366
France	203	2	653
Benelux	15	32	94
Germany-N	69	11	236
Germany-S	61	-	217
Scandinavia	673	26	677
Iberia	190	-	556
Alpine	30	-	77
Italy	133	-	254
Eastern Europe-NW	276	-	512
Eastern Europe-NE	93	-	196
Eastern Europe-SW	78	-	218
Eastern Europe-SE	134	-	437

Note: We show aggregated values for property right reasons.

Table 5: Overview of biomass supply classes

Class	Biomass resources
Class 1	Tertiary waste residues
Class 2	Secondary agricultural and forestry residues
Class 3	Primary agricultural, forestry, and waste residues
Class 4	Forestry biomass and energy crops

future time periods as well. Moreover, we use 2012 values since it can be assumed that these include little shifting and shedding of demand by consumers (see also Mier and Weissbart (2018)). The estimates for country-specific annual electricity demand levels are taken from projections from the *e-HIGHWAY 2050 Project* (Bruninx et al., 2015) with a system-wide demand level of 4,324 TWh for 2050. This is consistent with the 4,300 TWh in the EC's "Trends to 2050" reference scenario (EC, 2013a) and translates into a demand growth of 34% compared to 2015 with 3,223 TWh. Regional growth rates are subject to great differences, ranging from a 25% reduction for Norway to a 311% increase in the case of Lithuania. Moreover, growth patterns between 2015 and 2050 are assumed to follow a linear path. An overview of 2015 and 2050 demand levels with growth rates is given in Table J.15 in Appendix Appendix J. However, due to the electrification of other sectors, it can be assumed that electricity demand increases even stronger. The EC assumes in his impact assessment on the "[...] policy framework for climate and energy in the period from 2020 up to 2030" that electricity generation reaches a level of 5,050 TWh in 2050 (EC, 2014). Thus, we scale growth rates from Bruninx et al. (2015) to reach this demand level and use this electricity demand path as an alternative.

Transmission

For variable costs of electricity exchange between regions, we assume costs of 0.5 €/MWh. Similar to Schaber et al. (2012), region-specific costs for capacity additions are calculated based on investment costs of 2.4 mio. €/km for a capacity of 6.4 GW and scaled to the distance of population centroids of two regions. Furthermore, we use a loss factor of 0.04 per 1000 km for trade flows between regions. Loss factors from intra-regional distribution are approximated from reported losses (Eurostat, 2014).

Values for existing transmission capacities, or net transfer capacities (NTC), between regions are based on the ENTSO-E NTC values (ENTSO-E, 2014b) and are shown in Table J.16 in Appendix Appendix J. The 16 GW of existing transfer capacity between both German regions are based on Bundesnetzagentur (2012, 2015). Moroever, as mentioned in Section 3, we assume upper bounds on new transmission capacity in each time period. Values are based on estimations from the ENTSO-E "10-Year Network Development Plan" ENTSO-E (2014a) and results of the *SUSPLAN Project* (de Joode et al., 2011) and extrapolated to future periods. As an example, Tables J.17 and J.18 in Appendix Appendix J show the investment limits for 2030 and 2050.

Carbon capture and storage

Upper bounds for the geologic storage of CO_2 are estimated from work done within the *EU GeoCapacity Project* (Vangkilde-Pedersen et al., 2009). We accumulate storage capacities of different geologic formations and countries into a single value for each model region (Table 6).

Table 6: Overview of limits for geologic storage of CO_2 [Gt CO_2]

Britain	*France*	*Benelux*	*Ger-N*	*Ger-S*	*Scanda*	*Iberia*
14.4	8.69	2.54	9.14	7.94	31.94	1.58
Alpine	*Italy*	*EE-NW*	*EE-NE*	*EE-SW*	*EE-SE*	-
-	6.55	5.51	0.44	3.61	11.37	-

8. Model application

The EU-REGEN model is able to implement policies addressing the various components of the power market. Based on the scenario-specific set-up, additional constraints on generation technologies, transmission infrastructure, the CO_2 emission budget, and CCS, among others, can be introduced. In the following, we present the set-up of a market-wide 80% and 95% CO_2 emission reduction scenario and show results for the development of system-wide generation mixes and generation capacities.

8.1. Scenario set-up

The *80% CO_2 emission reduction scenario* is based on the energy and climate policy brought forward by the EC. The long-run targets were specified by an 80% CO_2 emission reduction for the entire economy overall in 2050 (EC, 2011a,b). In the mid-run, a 40% reduction of CO_2 emissions is aimed for 2030 (EC, 2014). We implement these targets through annual CO_2 emission budgets. For the time steps in between, we assume a linearly decreasing CO_2 emission budget. Furthermore, we assume electricity demand to increase linearly to 5,050 TWh in 2050 (see Section 7).

However, the EC showed in its impact assessments, that the power market has to overreach the 80% CO_2 emission reduction target due to higher marginal abatement costs in other sectors (EC, 2014). Hence, we additionally present a *95% CO_2 emission reduction scenario*. Again, we implement this target by annual CO_2 emission budgets. We assume annual CO_2 emission budgets that decrease linearly from the 2015 level to a 95% CO_2 emission reduction in 2050.[31]

8.2. Results

Results for the cost-efficient generation path in the 80% CO_2 emissions reduction scenario are depicted in Figure 5a. The future generation mix for the European power market is driven by the interplay between wind and gas power. Wind power becomes the main generation technology with a generation share above 20% by 2030 and above 30% by 2050. The intermittency of its generation profile is compensated for by the increasing market penetration by flexible gas power generation technologies. Hence, gas power reaches a generation share above 25% by 2050. Other RES—biomass and photovoltaic power—play a minor role in this scenario. Only photovoltaic power gains a higher generation share by the end of the scenario horizon. The market share of the currently main dispatchable generation technologies, that is, coal, lignite, and nuclear power, decreases significantly. For coal and lignite power, this is driven by the high

[31] All CO_2 emission reduction targets are related to 1990 levels.

carbon content of the fuel, which contradicts the CO_2 emissions target in this scenario. However, both technologies still contribute to meeting demand in 2050. In terms of nuclear power, high investment costs do not allow for new investments in a cost-efficient path. Interestingly, biomass in combination with CCS (BECCS) already plays a role in this 80% scenario. The high generation share of gas power that compensates for the intermittence of RES comes at the cost of CO_2 emissions. Hence, the negative emissions from BECCS are still necessary to meet the climate target.

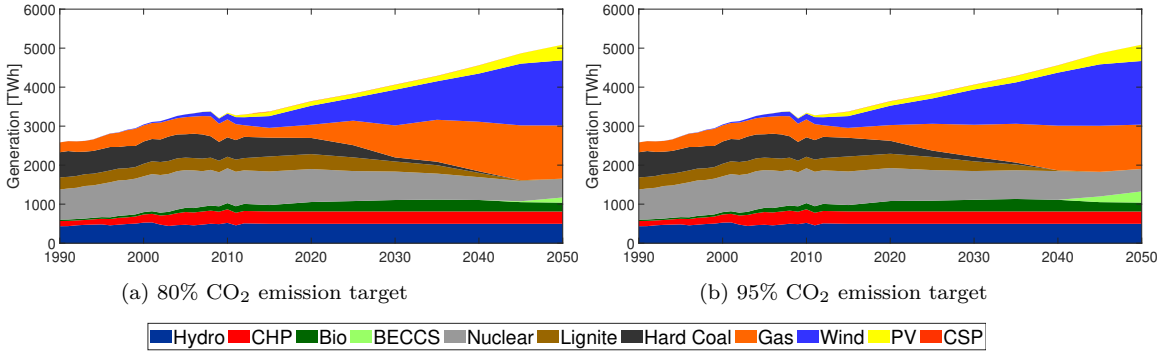

(a) 80% CO_2 emission target

(b) 95% CO_2 emission target

Figure 5: Long-run generation path with 80% and 95% CO_2 emission reduction target

Note: Both Figures further include the historic generation mix from 1990 to 2015.

The generation path in the 95% CO_2 emissions reduction scenario is shown in Figure 5b. Comparing the generation paths in both scenarios shows that there is one major channel, the substitution of gas power by BECCS, to reach the more ambitious target. The generation from gas power is reduced to a level below 22% by 2050. This is compensated for by the increased contribution of BECCS. In terms of emissions, the higher target is reached by reduced emissions from gas power, on the one hand, and the high negative emissions from BECCS, on the other hand. The generation from all other technologies does not change significantly between the two scenarios.[32]

[32] See Figures K.8a and K.8b in Appendix Appendix K for the cost-efficient capacity investment path for both scenarios.

9. Outlook

The EU REGEN provides a long-run dispatch and investment model for the European power market. The model contributes with a detailed representations of wind and solar electricity generation technologies, which are characterized by a spatially varying, intermittent supply pattern. This is implemented by introducing different quality classes for wind and solar resources in the competitive equilibrium setting of a partial-equilibrium power market model. Moreover, we provide in this paper a routine for processing meteorological parameters to capture the intermittency of RES.

Our results for the long-run market equilibrium show that, under an 80% CO_2 emissions reduction scenario until 2050, RES become the major group of technologies. Wind and photovoltaic power together reach a 2050 market share of approximately 40%. The intermittency of RES comes at the cost of an increasing market share of gas-powered technologies, which in turn results in emitting CO_2. Thus, the market entrance of biomass in combination with CCS is necessary to reach the CO_2 constraint in this scenario. Comparing this to a 95% CO_2 emissions reduction scenario, we find that BECCS, which has a negative emission intensity, substitutes CO_2-emitting gas power.

All in all, our findings suggest that even though accounting for the temporal and spatial characteristics of RES, the projected growth of RES is cost-efficient. The detailed depiction of their characteristics rather impacts the composition of the remaining supply stack, which mainly provides flexibility. However, our results should also be analyzed in view of the social phenomena connected to wind power. We showed in Section 2 that there is empirical evidence for the existence of a negative externality from the physical presence of wind turbines. Accordingly, apart from its cost prospects and meteorological characteristics, the dominating role of wind power crucially depends on to what extent regulators can manage its negative externalities, and resulting social acceptance issues.

References

Auffhammer, M. and E. T. Mansur (2014). Measuring climatic impacts on energy consumption: A review of the empirical literature. *Energy Economics 46*, 522–530.

Aune, F. R., R. Golombek, and H. H. Le Tissier (2015). Phasing out nuclear in Europe. *CREE Working Paper 05/2015*.

Bhattacharyya, S. C. and G. R. Timilsina (2010). A review of energy system models. *International Journal of Energy Sector Management 4*(4), 494–518.

Blanford, G. J., J. H. Merrick, J. E. Bistline, and D. T. Young (2018). Simulating annual variation in load, wind, and solar by representative hour selection. *The Energy Journal 39*(3), 189–212.

Blanford, G. J., J. H. Merrick, and D. Young (2014). A Clean Energy Standard Analysis with the US-REGEN Model. *The Energy Journal 35*, 137–164.

Boilley, A. and L. Wald (2015). Comparison between meteorological re-analyses from ERA-Interim and MERRA and measurements of daily solar irradiation at surface. *Renewable Energy 75*, 135–143.

Borenstein, S. (2008). The market value and cost of solar photovoltaic ectricity production. *Center for the Study of Energy Markets Working Paper 176*.

Borenstein, S. (2012). The private and public economics of renewable electricity generation. *Journal of Economic Perspectives 26*(1), 67–92.

Brovold, S. H., C. Skar, and O. B. Fosso (2014). Implementing hydropower scheduling in a European expansion planning model. *Energy Procedia 58*, 117–122.

Bruninx, K., D. Orlic, D. Couckuyt, N. Grisey, B. Betraoui, T. Anderski, Y. Surmann, N. T. Franck, G. Keane, B. Hickman, D. Huertas-Hernando, M. Wilk, and R. Jankowski (2015). Modular development plan of the Pan-European transmission system 2050: Data sets of scenarios for 2050. Technical report, The e-HIGHWAY 2050 Project.

Bundesnetzagentur (2012). Netzenwicklungsplan Strom 2012. Technical report, Bundesnetzagentur, Berlin.

Bundesnetzagentur (2015). EnLAG-Monitoring: Stand des Ausbaus nach dem Energieleitungsausbaugesetz zum ersten Quartal 2015. Technical report, Bundesnetzagentur, Berlin.

Cannon, D., D. Brayshaw, J. Methven, P. Coker, and D. Lenaghan (2015). Using reanalysis data to quantify extreme wind power generation statistics: A 33 year case study in Great Britain. *Renewable Energy 75*, 767–778.

Chiabrando, R., E. Fabrizio, and G. Garnero (2009). The territorial and landscape impacts of photovoltaic systems: Definition of impacts and assessment of the glare risk. *Renewable and Sustainable Energy Reviews 13*(9), 2441–2451.

Connolly, D., H. Lund, B. V. Mathiesen, and M. Leahy (2010). A review of computer tools for analysing the integration of renewable energy into various energy systems. *Applied Energy 87*(4), 1059–1082.

Cook, J., D. Nuccitelli, S. A. Green, M. Richardson, B. Winkler, R. Painting, R. Way, P. Jacobs, and A. Skuce (2013). Quantifying the consensus on anthropogenic global warming in the scientific literature. *Environmental Research Letters 8*(2), 024024.

Cook, J., N. Oreskes, P. T. Doran, W. R. L. Anderegg, B. Verheggen, E. W. Maibach, J. S. Carlton, S. Lewandowsky, A. G. Skuce, S. A. Green, D. Nuccitelli, P. Jacobs, M. Richardson, B. Winkler, R. Painting, and K. Rice (2016). Consensus on consensus: A synthesis of consensus estimates on human-caused global warming. *Environmental Research Letters 11*(4), 048002.

Coppens, C., H. Gordijn, M. Piek, P. Ruyssenaars, J.-J. Schrander, P. d. Smet, R. Swart, M. Hoogwijk, M. Papalexandrou, E. d. Visser, J. Horalek, P. Kurfürst, F. P. Jensen, B. S. Petersen, M. Harfoot, R. Milego, N.-E. Clausen, and G. Giebel (2009). Europe's onshore and offshore wind energy potential: An assessment of environmental and economic constraints. Technical report, European Environment Agency (EEA), Copenhagen.

Davis, L. W. (2011). The effect of power plants on local housing values and rents. *Review of Economics and Statistics 93*(4), 1391–1402.

de Joode, J., O. Ozdemir, K. Veum, A. van der Welle, G. Miglavacca, A. Zani, and A. L'Abbate (2011). Development of regional and Pan-European guidelines for more efficient integration of renewable energy into future infrastructure 'SUSPLAN'. Technical report, The SUSPLAN Project.

Deane, J., A. Chiodi, M. Gargiulo, and B. P. Ó Gallachóir (2012). Soft-linking of a power systems model to an energy systems model. *Energy 42*(1), 303–312.

Dröes, M. I. and H. R. Koster (2016). Renewable energy and negative externalities: The effect of wind turbines on house prices. *Journal of Urban Economics 96*, 121–141.

EC (2007). An energy policy for Europe. Technical report, European Commission (EC), Brussels.

EC (2011a). Energy roadmap 2050. Technical report, European Commission (EC), Brussels.

EC (2011b). Impact assessment: A roadmap for moving to a competitive low carbon economy in 2050. Technical report, European Commission (EC), Brussels.

EC (2013a). EU energy, transport and GHG emissions trends to 2050: Reference scenario 2013. Technical report, European Commission (EC), Brussels.

EC (2013b). On the future of carbon capture and storage in Europe. Technical report, European Commission (EC), Brussels.

EC (2014). Impact assessment: A policy framework for climate and energy in the period from 2020 to 2030. Technical report, European Commission (EC), Brussels.

EC (2018). A clean planet for all: A European strategic long-term vision for a prosperous, modern, competitive and climate neutral economy. Technical report, European Commission (EC), Brussels.

Edenhofer, O., L. Hirth, B. Knopf, M. Pahle, S. Schlömer, E. Schmid, and F. Ueckerdt (2013). On the economics of renewable energy sources. *Energy Economics 40*(Supplement 1), 12–23.

Egerer, J., C. von Hirschhausen, J. Weibezahn, and C. Kemfert (2015). Energiewende und Strommarktdesign: Zwei Preiszonen für Deutschland sind keine Lösung. *DIW Wochenbericht 9*, 183–190.

Egerer, J., J. Weibezahn, and H. Hermann (2016). Two price zones for the German electricity market — Market implications and distributional effects. *Energy Economics 59*, 365–381.

Elbersen, B., I. Startisky, G. Hengeveld, and M.-J. Schelhass (2012). Atlas of EU biomass potentials: Spatially detailed and quantified overview of EU biomass potential taking into account the main criteria determining biomass availability from different sources. Technical report, The Biomass Futures Project.

Energy Exemplar (2018). Plexos for power systems. Technical report, Energy Exemplar, North Adelaide.

ENTSO-E (2014a). 10-year network development plan 2014. Technical report, European Network of Transmission System Operators for Electricity (ENTSO-E), Brussels.

ENTSO-E (2014b). Hourly load values for all countries for a specific month. *URL: https://www.entsoe.eu/db-query/consumption/mhlv-all-countries-for-a-specific-month (accessed: December 7, 2014).*

ENTSO-E (2014c). Net Transfer Capacity (NTC) values summer 2010. *URL: https://www.entsoe.eu/publications/market-reports/ntc-values/Pages/default.aspx (accessed: November 30, 2014).*

Eurostat (2014). Supply, transformation and consumption of electricity: Annual data. *http://appsso.eurostat.ec.europa.eu/nui/show.do?dataset=nrg_105a (accessed: January 28, 2015).*

Eurostat (2018). Electricity production capacities for renewables and wastes. *URL: http://appsso.eurostat.ec.europa.eu/nui/show.do?dataset=nrg_inf_epcrw&lang=en (accessed: August 13, 2018).*

Fischer, C. and R. G. Newell (2008). Environmental and technology policies for climate mitigation. *Journal of Environmental Economics and Management 55*(2), 142–162.

Foley, A. M., B. P. Ó Gallachóir, J. Hur, R. Baldick, and E. J. McKeogh (2010). A strategic review of electricity systems models. *Energy 35*(12), 4522–4530.

Fouquet, R. (2016). Path dependence in energy systems and economic development. *Nature Energy 1*(8), 16098.

Frondel, M., N. Ritter, C. M. Schmidt, and C. Vance (2010). Economic impacts from the promotion of renewable energy technologies: The German experience. *Energy Policy 38*(8), 4048–4056.

Gamble, H. B. and R. H. Downing (1982). Effects of nuclear power plants on residential property values. *Journal of Regional Science 22*(4), 457–478.

Gibbons, S. (2015). Gone with the wind: Valuing the visual impacts of wind turbines through house prices. *Journal of Environmental Economics and Management 72*, 177–196.

Golombek, R., S. A. C. Kittelsen, and I. Haddeland (2012). Climate change: Impacts on electricity markets in western Europe. *Climatic Change 113*(2), 357–370.

Henning, H.-M. and A. Palzer (2014). A comprehensive model for the German electricity and heat sector in a future energy system with a dominant contribution from renewable energy technologies—Part I: Methodology. *Renewable and Sustainable Energy Reviews 30*, 1003–1018.

Hirth, L. (2013). The market value of variable renewables. *Energy Economics 38*, 218–236.

Huber, M. and C. Weissbart (2015). On the optimal mix of wind and solar generation in the future Chinese power system. *Energy 90*, 235–243.

Huld, T., M. Šúri, and E. D. Dunlop (2008). Comparison of potential solar electricity output from fixed-inclined and two-axis tracking photovoltaic modules in Europe. *Progress in Photovoltaics: Research and Applications 16*(1), 47–59.

IEA (2012). Energy prices and taxes 2012. Technical report, International Energy Agency (IEA), Paris.

IEA (2013). World energy outlook 2013. Technical report, International Energy Agency (IEA), Paris.

IEA (2018). CO_2 emissions from fuel combustion. Technical report, International Energy Agency (IEA), Paris.

IRENA (2016). The power to change: Solar and wind cost reduction potential to 2025. Technical report, International Renewable Energy Agency (IRENA), Abu Dhabi.

Joskow, P. L. (2011). Comparing the costs of intermittent and dispatchable electricity generating technologies. *American Economic Review 101*(3), 238–241.

Juruš, P., K. Eben, J. Resler, P. Krč, I. Kasanický, E. Pelikán, M. Brabec, and J. Hošek (2013). Estimating climatological variability of solar energy production. *Solar Energy 98*, 255–264.

Kalogirou, S. A. (Ed.) (2009). *Solar Energy Engineering*. Boston: Academic Press.

Knopf, B., P. Nahmmacher, and E. Schmid (2015). The European renewable energy target for 2030 – An impact assessment of the electricity sector. *Energy Policy 85*, 50–60.

Kost, C., J. N. Mayer, J. Thomsen, N. Hartmann, C. Senkpiel, S. Philipps, S. Nold, S. Lude, N. Saad, and T. Schlegl (2013). Levelized cost of electricity: Renewable energy technologies. Technical report, Fraunhofer Institute for Solar Energy Systems (ISE), Freiburg.

Krekel, C. and A. Zerrahn (2017). Does the presence of wind turbines have negative externalities for people in their surroundings? Evidence from well-being data. *Journal of Environmental Economics and Management 82*, 221–238.

Kunz, F. and A. Zerrahn (2016). Coordinating cross-country congestion management: Evidence from central Europe. *DIW Discussion Papers 1551*.

Lamont, A. D. (2008). Assessing the long-term system value of intermittent electric generation technologies. *Energy Economics 30*(3), 1208–1231.

Lunde, P. J. (1980). *Solar thermal engineering: Space heating and hot water systems*. New York: Wiley.

Mantzos, L. and P. Capros (1998). The PRIMES version 2 energy system model: Design and features. Technical report, National Technical University of Athens, Athens.

Marcel Šúri, Thomas A. Huld, Ewan D. Dunlop, and Heinz A. Ossenbrink (2007). Potential of solar electricity generation in the European Union member states and candidate countries. *Solar Energy 81*(10), 1295–1305.

Masters, G. M. (2004). *Renewable and efficient electric power systems*. Hoboken, NJ: Wiley.

Mattmann, M., I. Logar, and R. Brouwer (2016a). Hydropower externalities: A meta-analysis. *Energy Economics 57*, 66–77.

Mattmann, M., I. Logar, and R. Brouwer (2016b). Wind power externalities: A meta-analysis. *Ecological Economics 127*, 23–36.

Mideksa, T. K. and S. Kallbekken (2010). The impact of climate change on the electricity market: A review. *Energy Policy 38*(7), 3579–3585.

Mier, M. and C. Weissbart (2018). Power markets in transition: Decarbonization, energy efficiency, and short-term demand response. *ifo Working Paper 284*.

Nahmmacher, P., E. Schmid, and B. Knopf (2014). Documentation of LIMES-EU - A long-term electricity system model for Europe. Technical report, Potsdam Institute of Climate Impact Research (PIK), Potsdam.

NASA (2010). Modern-Era Retrospective analysis for Research and Applications (MERRA). Technical report, National Aeronautics and Space Administration (NASA) Goddard Earth Sciences Data and Information Services Center (GES DISC), Greenbelt.

Olauson, J. and M. Bergkvist (2015). Modelling the Swedish wind power production using MERRA reanalysis data. *Renewable Energy 76*, 717–725.

Owen, A. D. (2004). Environmental externalities, market distortions and the economics of renewable energy technologies. *The Energy Journal 25*(3), 127–156.

Platts (2013). UDI World Electric Power Plants Data-Base (v. 2013). *(accessed: September 10, 2014)*.

Pryor, S. C. and R. J. Barthelmie (2010). Climate change impacts on wind energy: A review. *Renewable and Sustainable Energy Reviews 14*(1), 430–437.

Richter, J. (2011). DIMENSION: A dispatch and investment model for European electricity markets. *EWI Working Paper 11/03*.

Ridley, B., J. Boland, and P. Lauret (2010). Modelling of diffuse solar fraction with multiple predictors. *Renewable Energy 35*(2), 478–483.

Rienecker, M. M., M. J. Suarez, R. Gelaro, R. Todling, J. Bacmeister, E. Liu, M. G. Bosilovich, S. D. Schubert, L. Takacs, G.-K. Kim, S. Bloom, J. Chen, D. Collins, A. Conaty, A. da Silva, W. Gu, J. Joiner, R. D. Koster, R. Lucchesi, A. Molod, T. Owens, S. Pawson, P. Pegion, C. R. Redder, R. Reichle, F. R. Robertson, A. G. Ruddick, M. Sienkiewicz, and J. Woollen (2011). MERRA: NASA's Modern-Era Retrospective Analysis for Research and Applications. *Journal of Climate 24*(14), 3624–3648.

Rübbelke, D. and S. Vögele (2011). Impacts of climate change on European critical infrastructures: The case of the power sector. *Environmental Science & Policy 14*(1), 53–63.

Samadi, S. (2017). The social costs of electricity generation – Categorising different types of costs and evaluating their respective relevance. *Energies 10*(3), 356.

Savvidis, G., K. Siala, C. Weissbart, L. Schmidt, F. Borggrefe, S. Kumar, K. Pittel, R. Madlener, and K. Hufendiek (2019). The gap between energy policy challenges and model capabilities. *Energy Policy 125*, 503–520.

Schaber, K., F. Steinke, and F. Hamacher (2012). Transmission grid extensions for the integration of variable renewable energies in Europe: Who benefits where? *Energy Policy 43*, 123–135.

Schmid, E. and B. Knopf (2015). Quantifying the long-term economic benefits of European electricity system integration. *Energy Policy 87*, 260–269.

Schröder, A., F. Kunz, J. Meiss, R. Mendelevitch, and C. von Hirschhausen (2013). Current and prospective costs of electricity generation until 2050. *DIW Discussion Papers 68*.

Schröder, A., T. Traber, and C. Kemfert (2013). Market driven power plant investment perspectives in Europe: Climate policy and technology scenarios until 2050 in the model EMELIE-ESY. *Climate Change Economics 04*(supp01), 1340007.

Steckel, J. C., O. Edenhofer, and M. Jakob (2015). Drivers for the renaissance of coal. *Proceedings of the National Academy of Sciences 112*(29), E3775–E3781.

Stoft, S. (2002). *Power system economics: Designing markets for electricity*. Piscataway, NJ and New York: Wiley-IEEE Press.

Teufel, F., M. Miller, M. Genoese, and W. Fichtner (2013). Review of system dynamics models for electricity market simulations. *Working Paper in Production and Energy 2*.

Vangkilde-Pedersen, T., K. L. Anthonsen, N. Smith, K. Kirk, F. Neele, B. van der Meer, Y. Le Gallo, D. Bossie-Codreanu, A. Wojcicki, Y.-M. Le Nindre, C. Hendriks, F. Dalhoff, and N. Peter Christensen (2009). Assessing European capacity for geological storage of carbon dioxide – The EU GeoCapacity project. *Energy Procedia 1*, 2663–2670.

Wind Europe (2017). Wind in power: 2016 European statistics. Technical report, Wind Europe, Brussels.

World Nuclear Association (2014). Country profiles. *URL: http://www.world-nuclear.org/information-library/country-profiles.aspx (accessed: November 29, 2014)*.

Young, D., G. Blanford, J. Merrick, V. Niemeyer, S. Rose, F. d. La Chesnaye, R. Bedilion, and T. Wilson (2013). PRISM 2.0: Regional energy and economic model development and initial application: US-REGEN model documentation. Technical report, Electric Power Research Institute (EPRI), Pao Alto.

Appendix A. Nomenclature of numerical implementation

Table A.7: Nomenclature of model description

Symbol	Explanation
Sets	
$s \in \mathcal{S}$	Load segments
$t \in \mathcal{T}$	Time periods
$r \in \mathcal{R}$	Regions
$i \in \mathcal{I}$	Generation technologies
$j \in \mathcal{J}$	Storage technologies
$v \in \mathcal{V}$	Vintages
$f \in \mathcal{F}$	Fuel types
$n \in \mathcal{N}$	Natural gas supply classes
$b \in \mathcal{B}$	Biomass supply classes
Variables	
c^{tot}	Total system costs
$c^{\text{gc}}_{r,t}$	Investment costs for generation capacity
$c^{\text{tc}}_{r,t}$	Investment costs for transmission capacity
$c^{\text{sc}}_{r,t}$	Investment costs for storage capacity
$c^{\text{vc}}_{r,t}$	Operational costs for generation
$c^{\text{fom}}_{r,t}$	Maintenance costs for generation
$c^{\text{tvo}}_{r,t}$	Operation costs for transmission
$c^{\text{tfm}}_{r,t}$	Maintenance costs for transmission
tf_t	Investment tax factor
$gc^{\text{new}}_{i,r,t}$	New generation capacity
$tc^{\text{new}}_{r,rr,t}$	New transmission capacity
$sc^{\text{new}}_{j,r,t}$	New storage capacity
$mc_{i,r,t}$	Variable operational costs
$g_{s,i,v,r,t}$	Generation
$bs_{b,r,t}$	Biomass supply
$e_{s,r,rr,t}$	Electricity exchange
$gc_{i,v,r,t}$	Accumulated generation capacity
$tc_{r,rr,t}$	Accumulated transmission capacity
$sd_{s,j,r,t}$	Storage discharge
$s_{s,j,r,t}$	Storage charge
$tg_{i,v,r,t}$	Total generation
$cs_{r,t}$	Stored carbon
nbc_t	Amount of net banked carbon credits
cbc_t	Cumulative banked credits
Parameters	
TK	Investment tax rate
YR_t	Number of years since last time period
DF_t	Discount factor
$\text{IC}^{\text{gc}}_{i,t}$	Investment costs
$\text{LF}_{i,v,r,t}$	Life-time factor
$\text{IC}^{\text{tc}}_{r,rr}$	Investment costs for transmission capacity
$\text{IC}^{\text{sc}}_{j}$	Investment costs of storage
H_s	Number of represented hours
$\text{OC}^{\text{bio}}_{b,r}$	Operational costs for biomass supply
$\text{OC}^{\text{vom}}_{i,v,r}$	Operational costs
$\text{FC}_{i,f}$	Fuel costs
$\text{HR}_{i,v,f,r}$	Heat rate
$\text{FT}_{f,t}$	Time period-specific heat rate adjustment factor
$\text{FR}_{f,r}$	Region-specific heat rate adjustment factor
$\text{EM}_{i,v,r}$	Emission intensity
PC_t	Carbon permit price

Continued on next page

Table A.7 – *Continued from previous page*

Symbol	Explanation
$OC^{fom}_{i,r}$	Fixed operational costs
$OC^{tvo}_{r,rr}$	Operational costs for transmission
$OC^{tfm}_{r,rr,t}$	Maintenance costs for transmission
$PS_{s,r}$	Self-consumption of hydro pump storage
$D_{s,r,t}$	Demand
ϵ	Loss from storage discharge
δ	Loss from intra-regional distribution
$PEN^{tr}_{r,rr}$	Loss from transmission
$E^{int}_{s,r}$	Export to outside regions
$AF_{s,i,r}$	Availability factor
$CF_{s,i,r}$	Capacity factor
DF_{s}	Minimum dispatch factor for nuclear power plants
$CAP^{gc}_{i,r,t}$	Capacity limit
$CAP^{geu}_{i,t}$	Accumulated capacity limit
$L_{i,v,r,t}$	Expected life time
RF_{i}	Retrofit factor
CR_{i}	Conversion factor
$CAP^{ret}_{i,r}$	Capacity limit on CCS conversions
$GC^{old}_{i,v,r}$	Existing generation capacity
SH_{j}	Fixed storage size
$CAP^{tc}_{r,rr,t}$	Capacity limit on transmission capacity additions
CAP^{teu}_{t}	Capacity limit on accumulated transmission capacity additions
$TL_{r,rr}$	Average transmission length
CR_{i}	Carbon capture rate
FC_{i}	Fuel coefficient
CC_{f}	Carbon content
CAP^{ccs}_{r}	Geologic storage limit
$QC_{i,r}$	Share of initial capacity
$CAP^{wind}_{i,r}$	Wind power capacity limit
$CAP^{solar}_{i,r}$	Wind power capacity limit
$BS_{b,r,t}$	Biomass supply
$GS_{g,r,t}$	Gas supply
CAP^{co2}_{t}	Limit on accumulated carbon emissions

Appendix B. Model resolution

Table B.8: Composition of model regions

Region	Countries
Britain	United Kingdom, Ireland (UK, IE)
France	France (FR)
Benelux	Belgium, Luxembourg, Netherlands (BE, LU, NL)
Germany-N	Northern Germany (GER)
Germany-S	Southern Germany (GER)
Scandinavia	Denmark, Finland, Norway, Sweden (DK, FI, NO, SE)
Iberia	Portugal, Spain (PT, ES)
Alpine	Austria, Switzerland (AT, CH)
Italy	Italy (IT)
Eastern Europe-NW	Czech Republic, Poland, Slovak Republic (CZ, PL, SK)
Eastern Europe-NE	Estonia, Latvia, Lithuania (EE, LV, LT)
Eastern Europe-SW	Croatia, Hungary, Slovenia (HR, HU, SI)
Eastern Europe-SE	Bulgaria, Greece, Romania (BG, EL, RO)

Table B.9: Overview of types of generation technologies

Technology type	Technology name
lign	Lignite
lbcf	Lignite-biomass conversion
lgcs	Lignite with CCS
hdcl	Hard Coal
cbcl	Coal-biomass conversion
clcs	Coal with CCS
igcc	Coal with CC
ngcc	Natural gas combined-cycle
ngst	Natural gas stream turbine
nggt	Natural gas gas turbine
ngcs	Natural gas with CCS
ptsg	Petroleum steam/gas turbine
chp-g	Combined-heat-power with natural gas
chp-p	Combined-heat-power with petroleum
biow	Biomass Waste
bioe	Dedicated bioenergy
becs	Dedicated bioenergy with CCS
geot	Geothermal
nuc	Nuclear
hydro	Hydro
wind-on	Wind onshore
wind-os	Wind offshore
pv	stationary photovoltaic
pv-tk	Tracking photovoltaic
csp	Concentrated solar

Appendix C. Resource classes

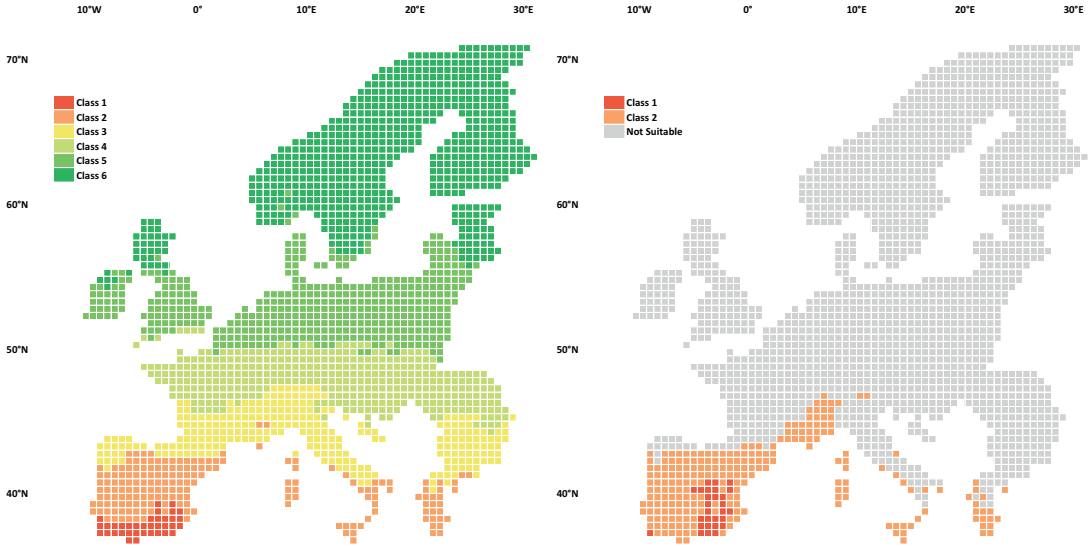

(a) Distribution of solar resource classes

(b) Distribution of CSP resource classes

Figure C.6: Solar resource data base

Appendix D. Nomenclature of wind power representation

Table D.10: Nomenclature of wind power

Symbol	Explanation
Sets	
$s \in \mathcal{S}$	Time segments
$l \in \mathcal{L}$	Location
$h \in \mathcal{H}$	Hub height
$G \in \mathcal{G}$	Wind turbine types
$q \in \mathcal{Q}$	Site quality classes
$r \in \mathcal{R}$	Region
$c \in \mathcal{C}_{\text{wind}}$	Wind resource quality class
Parameters	
$s_{s,l}^{\text{v50}}$	Northward wind speed 50 meter above ground
$s_{s,l}^{\text{u50}}$	Eastward wind speed 50 meter above ground
HE_h	Hub height value
$\text{R}_{s,l}$	Surface roughness length
A_g	Constant from power curve interpolation
$\lambda_g^1 - \lambda_g^6$	Coefficients from power curve interpolation
s_g^{up}	Upper wind speed limit
s_g^{low}	Lower wind speed limit
$W_{l,r}^{\text{wc}}$	Existing capacity distribution
$W_{h,g,q,r}^{\text{wt}}$	Existing technology mix
$W_{h,q,r}^{\text{hub}}$	Assumed hub height mix
$W_{h,r}^{\text{q}}$	Assumed quality class mix
σ^u	General wind turbine loss factor
σ_s^p	Seasonal wind turbine loss factor
Variables	
$s_{s,l}^{50}$	Wind speed vector 50 meter above ground
$s_{s,l,h}$	Extrapolated wind speed
$wp_{s,l,h,g}^{\text{trb}}$	Normalized wind power output
$wp_{s,h,q,r}^{\text{hub}}$	Weighted normalized onshore wind power output
$wp_{s,r}^{on}$	Final existing onshore wind power output
$wp_{s,h,r}^{\text{hub-os}}$	Weighted normalized offshore wind power output
$wp_{s,r}^{os}$	Final existing offshore wind power output
$wp_{s,r,c,h,g}^{reg}$	Wind power output for quality classes
$wp_{s,r,c}$	Final new wind power output

Appendix E. Model for wind power output

In this appendix, we explain the translation of the two-dimensional wind speed vector to normalized wind power output. The estimation of wind power output uses wind speed, displacement height, and surface roughness as input parameters. We combine the wind speed at each location l and time segment s from two directions ($s^{\mathrm{v50}}_{s,l}$ and $s^{\mathrm{u50}}_{s,l}$) to a single one $s^{50}_{s,l}$ by Equation (E.1):

$$s^{50}_{s,l} = \sqrt{s^{\mathrm{v50}}_{s,l} + s^{\mathrm{u50}}_{s,l}} \qquad \forall s \in \mathcal{S}, l \in \mathcal{L} \tag{E.1}$$

In the following, we use a portfolio approach for a better approximation of observed generation profiles. Based on the Monin-Obukhov specification, we extrapolate wind speeds at each location to different hub heights h, with the value of each hub height HE_h and the surface roughness length $\mathrm{R}_{s,l}$, as depicted in Equation (E.2):

$$s_{s,l,h} = s^{50}_{s,l} \cdot \left(\frac{log(\frac{\mathrm{HE}_h}{\mathrm{R}_{s,l}})}{log(\frac{50}{\mathrm{R}_{s,l}})} \right) \qquad \forall s \in \mathcal{S}, l \in \mathcal{L}, h \in \mathcal{H} \tag{E.2}$$

Then, wind speeds at hub heights are translated to normalized wind power output $wp^{\mathrm{trb}}_{s,l,h,g}$ for different wind turbines g by means of their respective power curves, which are shown in Figure E.7. The relationship between wind speed and power curve-specific output can be approximated by the function shown in Equation (E.3), which is an interpolation of the piecewise-defined power curve. The value of the parameters A_g, λ^1_g,...,λ^6_g are derived from this interpolation:

$$\begin{aligned} wp^{\mathrm{trb}}_{s,l,h,g} &= \mathrm{A}_g + \lambda^1_g \cdot s_{s,l,h} + (\lambda^2_g \cdot s_{s,l,h})^2 + (\lambda^3_g \cdot s_{s,l,h})^3 + (\lambda^4_g \cdot s_{s,l,h})^4 \\ &+ (\lambda^5_g \cdot s_{s,l,h})^5 + (\lambda^6_g \cdot s_{s,l,h})^6 \qquad \forall s \in \mathcal{S}, l \in \mathcal{L}, h \in \mathcal{H}, g \in \mathcal{G} \end{aligned} \tag{E.3}$$

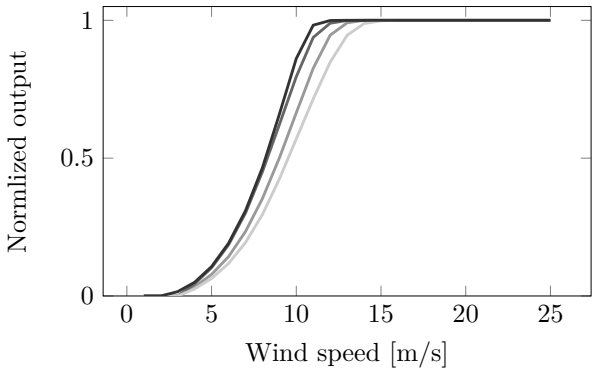

Figure E.7: Turbine power curves

Appendix F. Nomenclature of solar power representation

Table F.11: Nomenclature of solar power

Symbol	Explanation
Sets	
$s \in \mathcal{S}$	Time segments
$l \in \mathcal{L}$	Location
$r \in \mathcal{R}$	Region
$o \in \mathcal{O}$	Panel orientations
$p \in \mathcal{P}$	Panel tilts
$c \in \mathcal{C}_{\text{solar}}$	Solar resource quality class
Parameters	
E^{sc}	Solar constant
V_s	Day number of the year
LON_l	Longitude
LAT_l	Latitude
$LST_{s,l}$	Local solar time
$GHI_{s,l}$	Global horizontal irradiation
α^2_o	Panel orientation value
$\beta^2_{l,p}$	Panel tilt value
ρ	Reflection coefficient
T^r	Rated module temperature
$T_{s,l}$	Ambient temperature
η^r	Rated module efficiency
P^r	Rated power output
$W^{\text{sc}}_{l,r}$	Existing capacity distribution
$W^{\text{st}}_{o,p}$	Assumed orientation and panel tilt mix
$C^{\text{solar}}_{r,l,c}$	Resource class allocation
Variables	
$e^0_{s,l}$	Apparent extraterrestrial solar irradiation
$\beta^1_{s,l}$	Altitude angle
δ_s	Declination angle
$\omega_{s,l}$	Hour angle
$AST_{s,l}$	Apparent solar time
$LSTM_l$	Local longitude of standard time meridian
EOT_s	Equation of time
DV_s	Daily correction value
$k_{s,l}$	Clearness index
$d_{s,l}$	Share of diffuse irradiation
$dif_{s,l}$	Diffuse irradiation
$dni_{s,l}$	Direct normal irradiation
$\alpha^1_{s,l}$	Azimuth angle
$\theta_{s,l}$	Collector angle
$r^{tot}_{s,l,o,p}$	Solar irradiation at module
$r^{d}_{s,l,o,p}$	Direct component of solar irradiation at module
$r^{dif}_{s,l,p}$	Diffuse-scattered component of solar irradiation at module
$r^{ref}_{s,l,p}$	Reflected component of solar irradiation at module
$t^{pv}_{s,l,o,p}$	Actual module temperature
$\eta_{s,l,o,p}$	Panel efficiency
$sp^{pv}_{s,l,o,p}$	Actual module output
$\eta^{inv}_{s,l,o,p}$	Inverter efficiency
$sp_{s,l,o,p}$	Normalized solar power output by location
$sp^{reg}_{s,r,o,p}$	Normalized solar power output by region
$sp^{pv}_{s,r}$	Final existing pv power output
$sp^{pv}_{s,i,r}$	Final new pv power output

Appendix G. Separation of solar irradiation

In this appendix, we describe how the solar irradiation data from NASA (2010) can be separated into its direct and diffuse component. Modeling the output from solar power technologies requires, among others, a time series on the direct and diffuse irradiance. Most publicly available data, including MERRA, provides only GHI as a variable. Therefore, GHI has to be separated into the direct and diffuse part. For that purpose, as done in Juruš et al. (2013), we adopt the Boland-Ridley-Lauret model (Ridley et al., 2010), that estimates the share of diffuse irradiation from the clearness index. The methodology is based on the following main steps:

First, the seasonal variation of the apparent extraterrestrial solar irradiation[33] has to be estimated according to Equation (G.1) (Lunde, 1980):

$$e^0_{s,l} = E^{sc} \cdot \left(1 + 0.033 \cdot cos(\frac{V_s}{|S|} \cdot 360\check{r})\right) \cdot cos(\beta^1_{s,l}) \qquad \forall s \in \mathcal{S}, l \in \mathcal{L} \tag{G.1}$$

with the solar constant $E^{sc} = 1,367$[34], the number of time segment V_s, the total number of time segments $|S|$, and the altitude angle $\beta^1_{s,l}$.[35] The calculation of $\beta^1_{s,l}$ is based on Equations (G.2)–(G.8) and are explained in more detail in Masters (2004):

$$\beta^1_{s,l} = \sin^{-1}\left(\sin(\delta_s) \cdot \sin(LON_l) + \cos(\delta_h) \cdot \cos(LAT_l) \cdot \cos(\omega_{s,l})\right) \qquad \forall s \in \mathcal{S}, l \in \mathcal{L} \tag{G.2}$$

With longitude LON_l, latitude LAT_l, and declination angle δ_s for the northern hemisphere being defined as:

$$\delta_s = 23.45^\circ \cdot \sin\left(\frac{V_s + 6816}{|S|} \cdot 360^\circ\right) \qquad \forall s \in \mathcal{S} \tag{G.3}$$

an hour angle $\omega_{s,l}$ comprising:

$$\omega_{s,l} = 15^\circ \cdot (AST_{s,l} - 12) \qquad \forall s \in \mathcal{S}, l \in \mathcal{L}. \tag{G.4}$$

Furthermore, the following equations have to be considered to approximate the apparent solar time $AST_{s,l}$ by the local solar time $LST_{s,l}$, local longitude of standard time meridian $LSTM_l$, longitude LON_l, and equation of time EOT_s.

$$AST_{s,l} = LST_{s,l} + 4 \cdot (LSTM_l - LON_l) + EOT_s \qquad \forall s \in \mathcal{S}, l \in \mathcal{L} \tag{G.5}$$

[33] Seasonal variations result from the varying distance between the earth and the sun.

[34] The solar constant E^{sc} is the solar irradiation at a plane normal to the sun at the top of the atmosphere.

[35] The altitude angle $\beta^1_{s,l}$ is the vertical angle between the sun's rays and the horizon.

$$LSTM_l = 15° \cdot \frac{LON_l}{15°} \qquad \forall l \in \mathcal{L} \tag{G.6}$$

$$EOT_s = 9.87 \cdot \sin(2 \cdot DV_s) - 7.53 \cdot \cos(DV_s) - 1.5 \cdot \sin(DV_s) \qquad \forall s \in \mathcal{S} \tag{G.7}$$

$$DV_s = 360° \cdot \frac{V_s + 1944}{|S|} \qquad \forall s \in \mathcal{S} \tag{G.8}$$

Then, based on $e^0_{s,l}$, we can calculate the clearness index $k_{s,l}$[36] as the share of global horizontal irradiation $GHI_{s,l}$ in $e^0_{s,l}$ (Equation (G.9)) (Boilley and Wald, 2015):

$$k_{s,l} = \frac{GHI_{s,l}}{e^0_{s,l}} \qquad \forall s \in \mathcal{S}, l \in \mathcal{L} \tag{G.9}$$

which is then used in Equation (G.9) to estimate the share of diffuse irradiation $d_{s,l}$ in $GHI_{s,l}$ (Ridley et al., 2010):

$$d_{s,l} = \frac{1}{1 + e^{-5.0033 + 8.605 \cdot k_{s,l}}} \qquad \forall s \in \mathcal{S}, l \in \mathcal{L} \tag{G.10}$$

In a last step, we calculate diffuse irradiation (DIF) $dif_{s,l}$ (Equation (G.11)) and direct normal irradiation (DNI) $dni_{s,l}$ (Equation (G.12)). With $dif_{s,l}$ as the product of $GHI_{s,l}$ and $d_{s,l}$:

$$dif_{s,l} = d_{s,l} \cdot GHI_{s,l} \qquad \forall s \in \mathcal{S}, l \in \mathcal{L} \tag{G.11}$$

and $dni_{s,l}$ being additionally adjusted for the altitude angle:[37]

$$dni_{s,l} = \frac{(1 - d_{s,l}) \cdot GHI_{s,l}}{\sin(\beta^1_{s,l})} \qquad \forall s \in \mathcal{S}, l \in \mathcal{L} \tag{G.12}$$

[36] The clearness index $k_{s,l}$ is a measures for the clearness of the atmosphere. A value of 0.7 indicates a clear sky (Boilley and Wald, 2015).

[37] GHI measures only the horizontal, i.e., perpendicular to the earth's surface, irradiation. To additionally account for the non-horizontal irradiation in DNI, we adjust for the altitude angle.

Appendix H. Model for photovoltaic power output

In this appendix, we depict the translation of solar irradiation into normalized solar power output. With the separation of GHI into the DIF and DNI component in Appendix Appendix G, irradiation data can be converted into generation profiles for PV, PV-TK, and CSP technologies (Masters, 2004). We start off by calculating the azimuth angle $\alpha^1_{s,l}$ according to Equation (H.1):[38]

$$\alpha^1_{s,l} = \cos^{-1}\left(\frac{\sin(\delta_s)\cdot\cos(LAT_l) - \cos(\delta_s)\cdot\sin(LAT_l)\cdot\cos(\omega_{s,l})}{\cos(\beta^1_{s,l})}\right) \qquad \forall s \in \mathcal{S}, l \in \mathcal{L} \tag{H.1}$$

This feeds into the calculation of the collector angle $\theta_{s,l}$ in (Equation (H.2)).[39] In analogy to wind power, we apply a portfolio approach and calculate output values for different panel orientations o with the parameter α^2_o and tilts p represented by $\beta^2_{l,p}$:[40]

$$\theta_{s,l,o,p} = \cos(\beta^1_{s,l})\cdot\sin(\beta^2_{l,p})\cdot\cos(\alpha^1_{s,l}-\alpha^2_l)+\sin(\beta^1_{s,l})\cdot\cos(\beta^2_{l,p}) \qquad \forall s \in \mathcal{S}, l \in \mathcal{L}, o \in \mathcal{O}, p \in \mathcal{P} \tag{H.2}$$

This allows for calculating the solar irradiation at the module $r^{tot}_{s,l,o,p}$ (Equation (H.3)), that is composed of the direct component $r^d_{s,l,o,p}$, diffuse-scattered component $r^{dif}_{s,l,p}$, and reflected component $r^{ref}_{s,l,p}$.

$$r^{tot}_{s,l,o,p} = r^d_{s,l,o,p} + r^{dif}_{s,l,p} + r^{ref}_{s,l,p} \qquad \forall s \in \mathcal{S}, l \in \mathcal{L}, o \in \mathcal{O}, p \in \mathcal{P} \tag{H.3}$$

$$r^d_{s,l,o,p} = dni_{s,l}\cdot\theta_{s,l,o,p} \qquad \forall s \in \mathcal{S}, l \in \mathcal{L}, o \in \mathcal{O}, p \in \mathcal{P} \tag{H.4}$$

$$r^{dif}_{s,l,p} = dif_{s,l}\cdot\frac{1+cos(\beta^2_{l,p})}{2} \qquad \forall s \in \mathcal{S}, l \in \mathcal{L}, p \in \mathcal{P} \tag{H.5}$$

$$r^{ref}_{s,l,p} = dni_{s,l}\cdot\rho\cdot\left(\frac{dif_{s,l}}{dni_{s,l}} + \sin(\beta^1_{s,l})\right)\cdot\frac{1-cos(\beta^2_{l,p})}{2} \qquad \forall s \in \mathcal{S}, l \in \mathcal{L}, p \in \mathcal{P} \tag{H.6}$$

The reflection coefficient ρ has a default value of 0.2 for an ordinary ground (Masters, 2004), which is understood as area not covered with snow and, hence, has a lower reflection.

To get the actual feed-in profile, the solar irradiation at the module has to be adjusted for the panel efficiency, at first, and the inverter efficiency, in a second step. The panel efficiency is a function of the module's rated temperature T^r and the actual

[38] The azimuth angle $\alpha^1_{s,l}$ is the horizontal angle of the sun's rays relative to geographic north.

[39] The collector angle $\theta_{s,l}$ is the horizontal angle of the sun's rays to the panel.

[40] The panel orientation α^2_o indicates the facing relative to the north with $\alpha^2_o = 180°$ implying a south-facing panel.

module temperature $t^{pv}_{s,l,o,p}$, which can be estimated from the ambient temperature $T_{s,l}$ and the irradiation at the module as shown in Equations (H.7) and (H.8). The rated temperature, which is understood as the temperature at which the nominal power output is reached, is set to $T^r = 25°$ (Kalogirou, 2009). Higher module temperatures lead to a reduction in its output:

$$\eta_{s,l,o,p} = 1 - \gamma \cdot (t^{pv}_{s,l,o,p} - T^r) \qquad \forall s \in \mathcal{S}, l \in \mathcal{L}, o \in \mathcal{O}, p \in \mathcal{P} \tag{H.7}$$

$$t^{pv}_{s,l,o,p} = 30{+}0.0175{\cdot}(r^{tot}_{s,l,o,p}{-}300){+}1.14{\cdot}(T_{s,l}{-}25) \qquad \forall s \in \mathcal{S}, l \in \mathcal{L}, o \in \mathcal{O}, p \in \mathcal{P} \tag{H.8}$$

Then, we can calculate the actual module output $sp^{pv}_{s,l,o,p}$ (Equation (H.9)) by combining $\eta_{s,l,o,p}$, the rated module efficiency η^r, and the irradiation at the module $r^{tot}_{s,l,o,p}$

$$sp^{pv}_{s,l,o,p} = \eta_{s,l,o,p} \cdot \eta^r \cdot r^{tot}_{s,l,o,p} \qquad \forall s \in \mathcal{S}, l \in \mathcal{L}, o \in \mathcal{O}, p \in \mathcal{P} \tag{H.9}$$

and estimate the inverter efficiency $\eta^{inv}_{s,l,o,p}$. The efficiency of the conversion from direct current (DC) to alternating current (AC) is dynamic and increases concave downward with the module output $sp^{pv}_{s,l,o,p}$. Due to a lack of functional formulation of the inverter efficiency, we estimate it with the function shown in Equation (H.10):

$$\eta^{inv}_{s,l,o,p} = \left(\frac{0.5}{sp^{pv}_{s,l,o,p}} \right)^{\frac{1}{10}} \qquad \forall s \in \mathcal{S}, l \in \mathcal{L}, o \in \mathcal{O}, p \in \mathcal{P} \tag{H.10}$$

Finally, we can estimate the normalized solar power output $sp_{s,l,o,p}$ (normalized to the rated power output P^r) in Equation (H.11):

$$sp_{s,l,o,p} = \frac{\eta^{inv}_{s,l,o,p} \cdot sp^{pv}_{s,l,o,p}}{P^r} \qquad \forall s \in \mathcal{S}, l \in \mathcal{L}, o \in \mathcal{O}, p \in \mathcal{P} \tag{H.11}$$

Appendix I. Nomenclature of concentrated solar power representation

Table I.12: Nomenclature of CSP

Symbol	Explanation
Sets	
$s \in \mathcal{S}$	Time segments
$r \in \mathcal{R}$	Region
$i \in \mathcal{I}$	Generation technologies
Parameters	
$P_{s,r}$	Exogenous market prices
$dni_{s,i,r}$	Incoming direct solar irradiation
SM	Solar multiple
SH^{csp}	Storage capacity
ϵ^{csp}	Loss factor
Variables	
rev	Revenue
$g^{csp}_{s,i,r}$	CSP disptach
$s^{csp}_{s,i,r}$	CSP storage charge
$sd^{csp}_{s,i,r}$	CSP storage discharge
$sb^{csp}_{s,i,r}$	Accumulated CSP storage

Appendix J. Input data

Table J.13: Overview of lifetime, fixed, and variable O&M costs

Technology	Life time [Years]	Fixed O&M costs [€/kW]	Variable O&M costs [€/MWh]
lign	60	30	7
lbcf	60	-	-
lgcs	60	-	-
hdcl	30	6	-
cbcl	60	-	-
clcs	60	100	13
igcc	60	60	6
ngcc	40	20	4
ngst	60	20	4
nggt	40	15	3
ngcs	40	30	12
ptsg	60	20	3
chp-g	100	-	-
chp-p	100	-	-
biow	100	30	20
bioe	40	80	7
becs	40	120	14
geot	80	80	9
nuc	60	100	10
hydro	100	-	-
wind-on	30	35	0
wind-os	20	80	0
pv	20	25	0
pv-tk	20	30	0
csp	30	30	0

Table J.14: Overview of investment costs [€/kW]

	2020	2025	2030	2035	2040	2045	2050
hdcl	1,300	1,300	1,300	1,300	1,300	1,300	1,300
clcs	2,924	2,888	2,852	2,818	2,784	2,752	2,720
igcc	1,800	1,800	1,800	1,800	1,800	1,800	1,800
ngcc	800	800	800	800	800	800	800
nggt	400	400	400	400	400	400	400
ngcs	1,367	1,352	1,337	1,322	1,308	1,294	1,280
bioe	2,350	2,278	2,209	2,141	2,076	2,013	1,951
becs	4,000	3,800	3,600	3,400	3,300	3,200	3,100
geot	3,775	3,578	3,392	3,216	3,049	2,890	2,740
nuc	5,000	5,000	5,000	5,000	5,000	5,000	5,000
wind-on	1,240	1,210	1,182	1,154	1,127	1,101	1,075
wind-os	2,742	2,621	2,506	2,396	2,290	2,189	2,093
pv	1,100	1,000	950	900	850	800	750
pv	1,375	1,260	1,188	1,125	1,063	1,000	938
csp	4,500	4,050	3,645	3,463	3,290	3,125	2,969

Table J.15: Overview of final electricity demand projection [TWh]

Region	2015	2050	Growth rate
Austria	60	84	40%
Belgium	87	121	39%
Bulgaria	28	34	21%
Croatia	20	24	19%
Czech Republic	64	71	11%
Denmark	35	43	23%
Estonia	7	12	71%
Finland	89	84	-6%
France	459	657	43%
Germany	553	661	20%
Greece	60	67	12%
Hungary	36	60	67%
Ireland	28	42	50%
Italy	324	527	63%
Latvia	7	27	286%
Lithuania	9	37	311%
Luxembourg	8	8	0%
Netherlands	114	170	49%
Norway	150	112	-25%
Poland	126	160	27%
Portugal	49	75	53%
Romania	46	64	39%
Slovakia	29	28	-3%
Slovenia	14	14	0%
Spain	275	529	92%
Sweden	136	127	-7%
Switzerland	55	97	78%
United Kingdom	356	389	9%

Table J.16: Overview of existing transfer capacities between regions [GW]

	Britain	*France*	*Benelux*	*Ger-N*	*Ger-S*	*Scanda*	*Iberia*	*Alpine*	*Italy*	*EE-NW*	*EE-NE*	*EE-SW*	*EE-SE*
Britain	-	2	1	-	-	-	-	-	-	-	-	-	-
France	2	-	3.4	-	2.7	-	1.3	3.2	2.58	-	-	-	-
Benelux	1	2.3	-	3	-	0.7	-	-	-	-	-	-	-
Ger-N	-	-	3.85	-	16	2.15	-	-	-	1.2	-	-	-
Ger-S	-	-	0.98	16	-	-	-	3.7	-	0.8	-	-	-
Scanda	-	-	0.7	2.70	-	-	-	-	-	0.6	0.35	-	-
Iberia	-	0.5	-	-	-	-	-	-	-	-	-	-	-
Alpine	-	1.1	-	-	5.5	-	-	-	4.39	0.6	-	1.7	-
Italy	-	1	-	-	-	-	-	2.1	-	-	-	0.16	0.5
EE-NW	-	-	-	1.1	2.3	-	-	1	-	-	-	1.3	-
EE-NE	-	-	-	-	-	0.35	-	-	-	-	-	-	-
EE-SW	-	-	-	-	-	-	-	1.7	0.58	0.6	-	-	0.7
EE-SE	-	-	-	-	-	-	-	-	0.5	-	-	0.7	-

Table J.17: Overview of limits for investment in transfer capacities in 2030 [GW]

	Britain	*France*	*Benelux*	*Ger-N*	*Ger-S*	*Scanda*	*Iberia*	*Alpine*	*Italy*	*EE-NW*	*EE-NE*	*EE-SW*	*EE-SE*
Britain	-	-	0.16	-	-	0.7	-	-	-	-	-	-	-
France	-	-	-	-	-	-	0.7	-	-	-	-	-	-
Benelux	0.16	-	-	-	-	0.15	-	-	-	-	-	-	-
Ger-N	-	-	-	-	1	0.68	-	-	-	0.35	-	-	-
Ger-S	-	-	-	1	-	-	-	0.49	-	0.35	-	-	-
Scanda	0.7	-	0.45	0.39	-	-	-	-	-	-	1	-	-
Iberia	-	1.5	-	-	-	-	-	-	-	-	-	-	-
Alpine	-	0.5	-	-	-	-	-	-	-	0.7	-	-	-
Italy	-	0.3	-	-	-	-	-	0.86	-	-	-	1.42	-
EE-NW	-	-	-	0.4	-	-	-	0.75	-	-	0.5	0.2	-
EE-NE	-	-	-	-	-	1	-	-	-	0.5	-	-	-
EE-SW	-	-	-	-	-	-	-	-	0.99	0.45	-	-	-
EE-SE	-	-	-	-	-	-	-	-	-	-	-	-	-

Table J.18: Overview of limits for investment in transfer capacities in 2050 [GW]

	Britain	*France*	*Benelux*	*Ger-N*	*Ger-S*	*Scanda*	*Iberia*	*Alpine*	*Italy*	*EE-NW*	*EE-NE*	*EE-SW*	*EE-SE*
Britain	-	0.67	0.44	-	-	0.47	-	-	-	-	-	-	-
France	0.67	-	0.2	-	0.1	-	0.9	-	0.54	-	-	-	-
Benelux	0.44	0.27	-	0.83	-	0.33	-	-	-	-	-	-	-
Ger-N	-	-	0.83	-	1	1.17	-	-	-	0.63	-	-	-
Ger-S	-	-	-	1	-	-	-	1.56	-	0.5	-	-	-
Scanda	0.47	-	0.53	1.16	-	-	-	-	-	-	0.78	-	-
Iberia	-	1.17	-	-	-	-	-	-	-	-	-	-	-
Alpine	-	0.4	-	-	1.63	-	-	-	1.45	0.67	-	0.33	-
Italy	-	0.53	-	-	-	-	-	1.27	-	-	-	1	0.17
EE-NW	-	-	-	0.63	0.5	-	-	0.83	-	-	0.33	0.57	-
EE-NE	-	-	-	-	-	0.78	-	-	-	0.33	-	-	-
EE-SW	-	-	-	-	-	-	-	0.23	0.86	0.5	-	-	-
EE-SE	-	-	-	-	-	-	-	-	0.17	-	-	-	-

Appendix K. Capacity investment paths

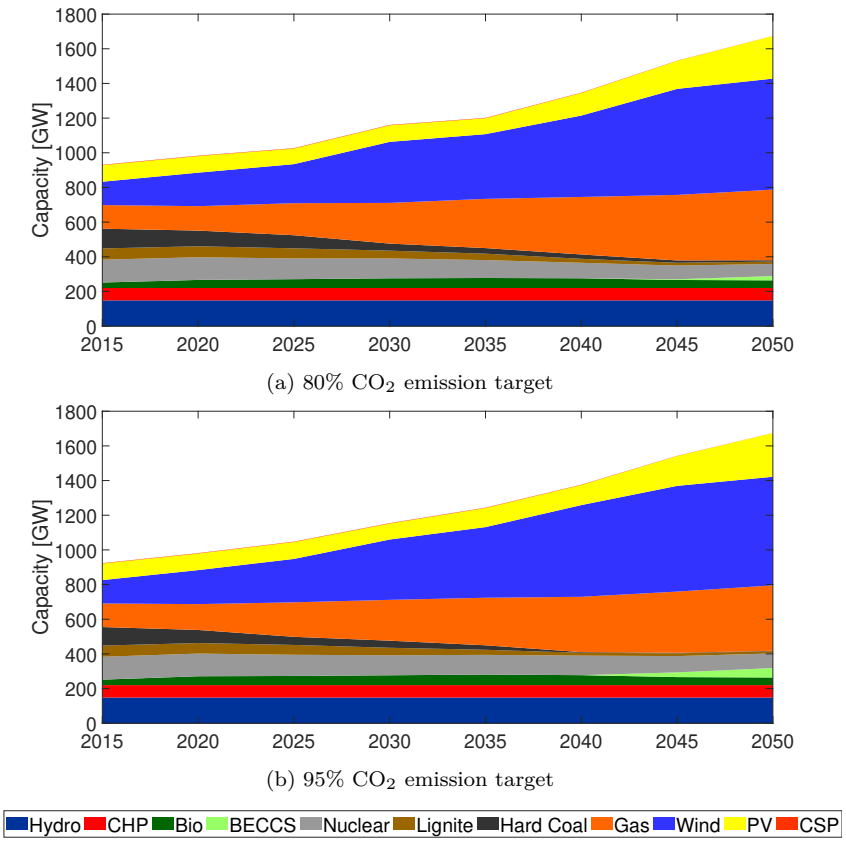

(a) 80% CO_2 emission target

(b) 95% CO_2 emission target

Figure K.8: Long-run capacity path with 80% and 95% CO_2 emission reduction target